NACA

RESEARCH MEMORANDUM

EFFECTS OF SPANWISE LOCATION OF SWEEP DISCONTINUITY ON THE LOW-SPEED LONGITUDINAL STABILITY CHARACTERISTICS OF A COMPLETE MODEL WITH WINGS OF M AND W PLAN FORM

By Paul G. Fournier

Langley Aeronautical Laboratory
Langley Field, Va.

CLASSIFIED DOCUMENT

NATIONAL ADVISORY COMMITTEE
FOR AERONAUTICS

WASHINGTON

January 20, 1955

NATIONAL ADVISORY COMMITTEE FOR AERONAUTICS

RESEARCH MEMORANDUM

EFFECTS OF SPANWISE LOCATION OF SWEEP DISCONTINUITY ON THE LOW-SPEED LONGITUDINAL STABILITY CHARACTERISTICS OF A COMPLETE MODEL WITH WINGS OF M AND W PLAN FORM

By Paul G. Fournier

SUMMARY

An investigation was made of the low-speed static longitudinal stability characteristics of a complete model having a series of M- or W-wings. These M- or W- wings were obtained through modification of a basic 45° swept wing and had several spanwise locations of sweep discontinuity. All wings were of aspect ratio 6 and taper ratio 0.6.

The results indicate that all the M- or W-wings provided improved tail-off high-lift longitudinal stability characteristics as compared with those of the basic swept wing. In general, the M-wings seem to provide more desirable stability characteristics at the moderate angles of attack (10° to 20°) than any of the W-wings except, perhaps, the W-wing having the sweep discontinuity at the midsemispan location. Moving the location of the sweep discontinuity inboard had little effect on the stability characteristics of the M-wings, but the high-lift stability characteristics of the W-wings improved as the spans of the sweptforward panels were increased.

With a horizontal tail mounted on the wing chord plane extended, it appeared that acceptable longitudinal stability characteristics could be obtained with either M- or W-wing configurations. Location of the tail at a height of about 21 percent of the wing semispan above the wing chord plane appeared undesirable for all plan forms investigated.

For the conditions of these tests, the drag due to lift of the M-wings was slightly lower than that of the basic swept wing; whereas the W-wings provided no consistent change in drag due to lift as compared with the basic wing.

INTRODUCTION

Results of previous investigations, for example, references 1 and 2, have shown that improvements in high-lift pitching-moment characteristics over those provided by swept wings can be obtained with wings of composite sweep; that is, wings made up of combinations of sweptback and sweptforward panels. In addition, interest in wings with composite sweep has arisen from some structural advantages inasmuch as, for the M- or W-wings, the overall effects of bending and torsion deformations tend to oppose each other; and therefore by adjusting the ratio of torsional to bending stiffness, for a given location of sweep discontinuity it should be possible to obtain desirable characteristics with regard to twist under load. (See ref. 3.) However, as illustrated in reference 4, the divergence speed for a given ratio of torsional stiffness to bending stiffness is critically dependent upon the location of the sweep discontinuity and, as would be expected, indicates that it is desirable to keep the sweptforward panel of the wing relatively small. That is, higher divergence speeds for M-wings are obtained by using break locations near the fuselage, whereas for W-wings break locations near the wing tips are more favorable. In the past, experimental investigations of composite (M and W) wings have been limited to wings having the sweep discontinuity at the midsemispan location. A major purpose of this investigation therefore is to determine how far inboard, in the case of the M-wings, and how far outboard, in the case of the W-wings, the break location can be moved while still maintaining favorable pitching-moment characteristics. The M-wings tested had break locations at 30-, 40-, or 50-percent semispan, and the W-wings had the breaks at 50-, 60-, or 70-percent semispan. Also included in this investigation is a comparison of the longitudinal stability characteristics at two tail heights: one (referred to as the low tail) located on the wing chord plane extended, and the other (referred to as the high tail) located 20.83 percent wing semispan above the wing chord plane extended.

The data presented in this paper were obtained from tests in the Langley 300 MPH 7- by 10-foot tunnel of a complete-model configuration having wings of M and W plan form and of a model having a basic 45° sweptback wing. All wings had aspect ratio 6, taper ratio 0.60, NACA 65A009 airfoil section parallel to the plane of symmetry, and $\pm 45^{\circ}$ panel sweep of the quarter-chord lines.

COEFFICIENTS AND SYMBOLS

The stability system of axes used for the presentation of the data and the positive direction of forces, moments, and angles are shown in figure 1. All moments are referred to the quarter-chord point of the wing mean aerodynamic chord.

[redacted]

A	aspect ratio
a.c.	aerodynamic-center location measured from leading edge of $\bar{c}$, percent $\bar{c}$
b	wing span, ft
C_D	drag coefficient, $C_D = -C_X$
ΔC_D	drag due to lift, $\Delta C_D = C_D - \left(C_D\right)_{C_{L=0}}$
C_L	lift coefficient, $\frac{\text{Lift}}{qS}$
C_{L_α}	wing lift-curve slope, per deg
C_m	pitching-moment coefficient, $\frac{\text{Pitching moment}}{qS\bar{c}}$
C_{m_t}	increment in pitching-moment coefficient caused by the horizontal tail
C_X	longitudinal-force coefficient, $\frac{\text{Longitudinal force}}{qS}$
$\bar{c}$	wing mean aerodynamic chord, ft
$\bar{c}_t$	horizontal-tail mean aerodynamic chord, ft
D	diameter of fuselage, inches
i_t	angle of incidence of horizontal tail with respect to fuselage center line, deg
l	length of body of revolution (fuselage), in.
l_t	tail length $\left(\text{distance from } \frac{\bar{c}}{4} \text{ to } \frac{\bar{c}_t}{4}\right)$, ft
q	free-stream dynamic pressure, $\frac{\rho V^2}{2}$, lb/sq ft
r	radii of body of revolution
S	wing area, sq ft

[redacted]

V	free-stream velocity, ft/sec
x	longitudinal coordinate of body of revolution
$\bar{x}$	chordwise distance from leading edge of root chord to $\frac{\bar{c}}{4}$, (positive rearward of leading edge), inches
y	lateral ordinate, ft
y^*	lateral location of sweep discontinuity, percent $\frac{b}{2}$
α	angle of attack, deg
ϵ	effective downwash angle at tail, deg
$\epsilon_\alpha = \frac{\partial \epsilon}{\partial \alpha}$	
$\Lambda_{c/4}$	sweep of the quarter-chord line, deg
ρ	mass density of air, slugs/cu ft

Notation of configurations:

Λ	basic sweptback wing
M and W	wings of composite sweep (used with subscript 30, 40, 50, 60, or 70 indicating spanwise location of sweep discontinuity in percent $b/2$)
T.O.	horizontal tail off

MODEL AND APPARATUS

For the present investigation, a series of seven wing plan forms were tested in combination with a fuselage and tail. The wings had an aspect ratio of 6, a taper ratio of 0.60, an NACA 65A009 airfoil section parallel to the plane of symmetry, and $\pm 45^\circ$ sweep of the quarter-chord line. Included were a sweptback wing (basic wing, $\Lambda c/4=45^\circ$), three M-wings, and three W-wings. The three M-wings had their sweep discontinuities located at 30-percent, 40-percent, or 50-percent semispan, and the three W-wings had sweep discontinuities at 50-percent, 60-percent, or 70-percent semispan and herein are designated as M_{30}, M_{40}, M_{50}, W_{60},

and W_{70} wings, respectively. The horizontal tail had an aspect ratio of 4, a taper ratio of 0.60, 45° sweepback of the quarter-chord line, and an NACA 65A006 airfoil section parallel to the plane of symmetry. The fuselage had a fineness ratio of 10.86, which was obtained by cutting off a portion of the rear of a fineness-ratio-12 body of revolution — the ordinates of which are presented in table I. The fuselage was constructed of wood and the wings were constructed of wood bonded to steel reinforcing spars. A three-view drawing of the model with a representative wing is shown in figure 2. A photograph of a typical complete-model configuration on the support strut is presented in figure 3.

All the wings tested in this investigation were in a midwing position and were mounted so that the quarter chord of the wing mean aerodynamic chord, about which all moments and forces were taken, was located at the same point on the fuselage for all the wings. Details of these wing plan forms are presented in figure 4. The model was constructed so that tests could be made with the horizontal tail at two tail heights. The high tail was located 20.83-percent wing semispan above the wing chord plane extended and the low tail was on the wing chord plane extended. All tests involving the wing-fuselage configuration were made with the vertical tail on.

The model was mounted on a single support strut which was in turn fastened to the mechanical balance system of the Langley 300 MPH 7- by 10-foot tunnel.

TESTS AND CORRECTIONS

All tests were made at a dynamic pressure of 45.22 pounds per square foot, which for average test conditions corresponds to a Mach number of about 0.17 and a Reynolds number of 1.27×10^6 based on the wing mean aerodynamic chord of 1.02 feet.

The angle-of-attack range was from approximately -4° to 32°. The angle of attack, longitudinal force (-drag), and horizontal-tail-on pitching moment have been corrected for jet-boundary effects, computed on the basis of unswept-wing theory by the method of reference 5. Reference 6 shows that the effect of sweep on these corrections is small. The dynamic pressure and drag coefficient have been corrected for blocking caused by the model and its wake by the method of reference 7.

Vertical buoyancy on the support strut, tunnel air-flow misalinement, and longitudinal pressure gradient have been accounted for in the computation of the test data. These data have not been corrected for the tares caused by the model support strut; however, tare tests of similar complete-model configurations have shown a correction to longitudinal force

coefficient of about 0.009 at zero lift and a correction to pitching-moment coefficient that was small and independent of angle of attack up to the higher angles.

No corrections for the effects of aeroelasticity have been applied to the data presented herein; however, some rough calculations were made to determine the magnitude of these effects for the basic sweptback wing. The results indicated that aeroelasticity probably caused about a 4-percent reduction in C_{L_α} and a forward displacement of the low-lift aerodynamic center of about 3 percent of the mean aerodynamic chord. The corresponding effects for the M- and W-wings would be expected to be smaller.

RESULTS AND DISCUSSION

Presentation of Results

The results of the present investigation are presented in the following figures:

	Figure
Basic data	5 to 12
Effect of break location on C_m	13
Effect of break location on drag due to lift	14
Summary plots	15 to 17

Pitching-Moment Characteristics

The pitching-moment characteristics included in the basic data (figs. 5 to 12) represent a center-of-gravity location at the $0.25\bar{c}$ location. The static margin therefore varied with wing plan form and with tail configuration. In order to provide comparisons of pitching-moment curves under fairly realistic conditions, the data have been recomputed with respect to a center-of-gravity location such that a static margin of $0.10\bar{c}$ is obtained for all configurations at zero lift.

Horizontal-tail-off configurations.- Comparison of the horizontal-tail-off configurations (fig. 13(a)) shows that all the M- and W-wings provided improved pitching-moment characteristics as compared with those of the basic sweptback wing at moderate lift coefficient and angles of attack. For the W-wings, as the span of the sweptforward panel was decreased by moving the break location outboard of $y^* = 50$ to $y^* = 70$ the pitching-moment characteristics became progressively poorer and approached those of the sweptback (Λ) wing. With the M-wings, however, decreasing the span of the sweptforward panel by moving the break location inboard of $y^* = 50$ to $y^* = 30$ had little effect on the pitching-moment characteristics and in general the M-wings provided more desirable

pitching-moment characteristics than the W-wings, with the possible exception of the W_{50}-wing. Although the pitching-moment characteristics of the W_{50}-wing are almost as favorable as those of any of the M-wings, the W_{50}-wing might not be as desirable structurally as some of the M-wings. As shown in reference 4, the break location (location of sweep reversal) is critical with regard to divergence speed and for a given ratio of torsional to bending stiffness, it is shown that higher divergence speeds can be obtained by keeping the sweptforward panel of the wing relatively small. The M-wings therefore show promise of meeting this structural requirement for high divergence speed without any adverse effect on the pitching-moment characteristics.

It should be remembered, however, that for the low-speed investigation reported herein, the wings tested are, for all practical purposes, rigid wings and the results shown might be appreciably different if aeroelastic effects were considered. Reference 3 has also shown that the ratio of torsional stiffness to bending stiffness has an appreciable effect on the streamwise twist due to aerodynamic loading of M- and W-wings.

Complete-model configurations.- In general the effects of spanwise variation in break location for the complete-model configurations are similar to those noted for the tail-off configurations for both tail heights investigated (figs. 13(b) and 13(c)). For the high-horizontal-tail configuration (fig. 13(b)), all the composite-plan-form wings provided improved pitching-moment characteristics as compared with those of the basic sweptback wing but still showed a loss in horizontal-tail effectiveness at moderate angles of attack (characteristic of configurations having the horizontal tail located above the wing chord plane). Lowering the horizontal tail to the wing chord plane extended improved the pitching-moment characteristics of all configurations investigated (fig. 13(c)) and provided a stable pitching-moment curve for several of the configurations. With the low horizontal tail, the W-wings provided a more nearly linear variation of pitching-moment coefficient with angle of attack than either the M or swept wings.

Drag Due to Lift

Comparison of the drag due to lift, ΔC_D, for the various wings may be made from the results presented in figure 14. Since drag tares were not evaluated in this investigation, it is considered that the use of drag due to lift provided a more reliable basis for evaluating performance characteristics of these wings than could be obtained from lift-drag ratios or from the total-drag polars. The results indicate that, for the present test conditions, either the M-wings or the W-wings provided essentially the same drag due to lift below about 0.5 lift coefficient. At higher lift

coefficients the M-wings consistently provided lower drag due to lift than the basic swept wing; however, the W-wings appeared to provide no consistent improvement or detrimental effect relative to the basic wing.

Aerodynamic Parameters at Zero Lift

The lift-curve slopes for the various horizontal-tail-off configurations (fig. 15) showed that both the M- and W-wings had slightly higher lift-curve slopes than the basic sweptback wing. Increasing the span of the sweptforward panel increased the lift-curve slope for either the M- or the W-wings, with the greatest effect being noted for the M-wings. These results are in fair agreement with wing-alone calculations (ref. 8) and wing-fuselage calculations (obtained by the basic method of ref. 9 together with ref. 8 to account for the effects of composite wing plan form).

The effect of break location on the aerodynamic center with horizontal tail off is presented in figure 16 along with calculated results for wing alone (ref. 8), wing-fuselage (basic method of ref. 9 together with ref. 8), and wing alone plus fuselage alone (refs. 8 and 10). The location of the aerodynamic center indicated by the wing-fuselage calculations (refs. 8 and 9) is in good agreement with the experimental tail-off results for the W-wings; but, for the sweptback and M-wings, the agreement is not quite so good, although the trend with break location appears to be in good agreement. The wing-fuselage calculations were found, as would be expected, to give a better prediction of the aerodynamic-center location than the wing-alone calculations (ref. 8).

A brief description of the method used in reference 9 to calculate lift curves and aerodynamic centers for wing-fuselage combinations may serve to explain some of the differences between measured and calculated values. In general, the method used in reference 9 is to estimate the load distribution on the fuselage and external wing by theoretical methods; whereas for the wing carry-through section (that part of the wing enclosed within the fuselage) a semiempirical method is used. It should be pointed out that the contribution of the wing carry-through section to the lift and moment and the factor K (which takes into account the effect of wing upwash on the loading on the forward part of the fuselage) presented in reference 9 were determined for unswept or sweptback wings. In calculating the lift and moment of the fuselage, the factor K of reference 9 had to be interpolated for the sweptforward portion of the M-wings and this may account for some of the descrepancy indicated in figure 16. The factor K for the W-wings was obtained directly from reference 9, since the sweptback portion of these wings was thought to have the greatest effect on the upwash of the forward portion of the fuselage. The contribution of the external wing was determined by the method of reference 8. Also in determining the aerodynamic center of the wing carry-through section, it will

be noted in figure 4(b) of reference 9 that the aerodynamic center for the wing carry-through section was aft of the aerodynamic center of the root chord of the sweptback wing considered. This shift in aerodynamic center is assumed to apply to either M- or W-wings; therefore, this incremental shift in aerodynamic center was added to the location of the aerodynamic center of the root chord of the various composite plan forms as determined from reference 8.

The downwash parameter of figure 17 was computed by the use of the equation,

$$\epsilon = \alpha + i_t - \frac{C_{m_t}}{dC_m/di_t}$$

using only the linear portion of the pitching-moment curves at low angles of attack. The variation of ϵ_α (fig. 17) shows that for the high-tail configuration there were rather small effects of the plan-form variations considered. For the low-tail configurations, however, some of the M-wings provided increased downwash over that of the basic wing; whereas the W-wings generally decreased the downwash slightly.

Possible Configurations of Airplanes with M- and W-Wings

Among the factors that govern the configuration of an airplane are the requirements for good stability, good performance, and compatibility of the design with the intended function of the airplane. This paper has dealt primarily with stability considerations, and it has been shown that the M and W plan forms provide some advantages over other wings in this respect.

The fact that the M and W plan forms provide regions at three spanwise locations (rather than only one for swept and delta wings) where the air flow is relatively symmetrical is considered to be an important feature with regard to performance capabilities and compatibility of the aircraft with its function. These regions of symmetrical flow (the wing panel junctures) may permit distribution of the power plants and payload both longitudinally and laterally in a more effective manner than is possible with other wings. Bodies at the panel junctures allow more depth for structure at these critical regions and properly shaped bodies may alleviate otherwise poor flow conditions. Location of power plants in nacelles at these junctures may also facilitate the design of boundary-layer control systems by blowing or suction. Some possible configurations are illustrated in figure 18.

The ability to distribute volume longitudinally is a useful feature in designing for a low drag rise at transonic speeds in that it facilitates

the achievement of a desirable area distribution, as indicated by the area-rule concept (ref. 11). This feature should compensate, in part at least, for the fact that a given sweep angle provides a somewhat smaller transonic drag reduction when applied to M- and W-wings than to swept wings (ref. 2).

The division of fuselage volume among three bodies located at the wing panel junctures may provide some advantages in the placement of engines and fuel in a manner to provide a minimum of aerodynamic interference. Some of the arrangements shown in figure 18 may also be beneficial in connection with the release of bombs or missiles at high speed.

CONCLUSIONS

A low-speed wind-tunnel investigation of a complete model configuration having M- and W-wings with varying location of the sweep discontinuity indicated the following conclusions:

1. All of the M- and W-wings provided improved tail-off high-lift longitudinal stability characteristics as compared with that of the basic sweptback wing. In general, the M-wings seem to provide more desirable stability characteristics at the moderate angles of attack (10° to 20°) than any of the W-wings with the possible exception of the W-wing having the sweep discontinuity at the midsemispan location. Moving the location of the sweep discontinuity inboard had little effect on the stability characteristics of the M-wings, but the high-lift stability characteristics of the W-wings improved as the spans of the sweptforward panels were increased.

2. With a horizontal tail mounted on the wing chord plane extended, the W-wings provided a more nearly linear variation of pitching moment with angle of attack than the M-wings, although it appeared that acceptable longitudinal stability characteristics could be obtained with either the M- or W-wing configurations. Location of the tail at a height of about 21 percent of the wing semispan above the wing chord plane appeared undesirable for all plan forms.

3. For the conditions of these tests, the drag due to lift of the M-wings was slightly lower than that of the basic swept wing; whereas the W-wings provided no consistent change in drag due to lift as compared with the basic wing.

4. In general, the characteristics at low lift coefficients could be predicted with resonable accuracy by means of available theory.

Langley Aeronautical Laboratory,
National Advisory Committee for Aeronautics,
Langley Field, Va., November 8, 1954.

[redacted]

REFERENCES

1. Polhamus, Edward C. and Becht, Robert E.: Low-Speed Stability Characteristics of a Complete Model With a Wing of W Plan Form. NACA RM L52A25, 1952.

2. Campbell, George S. and Morrison, William D.: A Small-Scale Investigation of "M" and "W" Wings at Transonic Speeds. NACA RM L50H25a, 1950.

3. Weil, Joseph, and Polhamus, Edward C.: Aerodynamic Characteristics of Wings Designed for Structural Improvement. NACA RM L51E10a, 1951.

4. Diederich, Franklin W., and Foss, Kenneth A.: Static Aeroelastic Phenomena of M-, W-, and Λ-Wings. NACA RM L52J21, 1953.

5. Gillis, Clarence L, Polhamus, Edward C., and Gray, Joseph L., Jr.: Charts for Determining Jet-Boundary Corrections for Complete Models in 7- by 10-Foot Closed Rectangular Wind Tunnels. NACA WR L-123, 1945. (Formerly ARR L5G31.)

6. Polhamus, Edward C.: Jet-Boundary-Induced-Upwash Velocities for Swept Reflection-Plane Models Mounted Vertically in 7- by 10-Foot, Closed, Rectangular Wind Tunnels. NACA TN 1752, 1948.

7. Herriot, John G.: Blockage Corrections for Three-Dimensional-Flow Closed-Throat Wind Tunnels, With Consideration of the Effect of Compressibility. NACA Rep. 995, 1950. (Supersedes NACA RM A7B28.)

8. Diederich, Franklin W., and Latham, W. Owen: Calculated Aerodynamic Loadings of M-, W-, and Λ-Wings in Incompressible Flow. NACA RM L51E29, 1951.

9. McLaughin, Milton D.: Method of Estimating the Stick-Fixed Longitudinal Stability of Wing-Fuselage Configurations Having Unswept or Swept Wings. NACA RM L51J23, 1952.

10. Munk, Max M.: The Aerodynamic Forces on Airship Hulls. NACA Rep. 184, 1924.

11. Whitcomb, Richard T.: A Study of the Zero-Lift Drag-Rise Characteristics of Wing-Body Combinations Near the Speed of Sound. NACA RM L52H08, 1952.

[redacted]

TABLE I

FUSELAGE ORDINATES

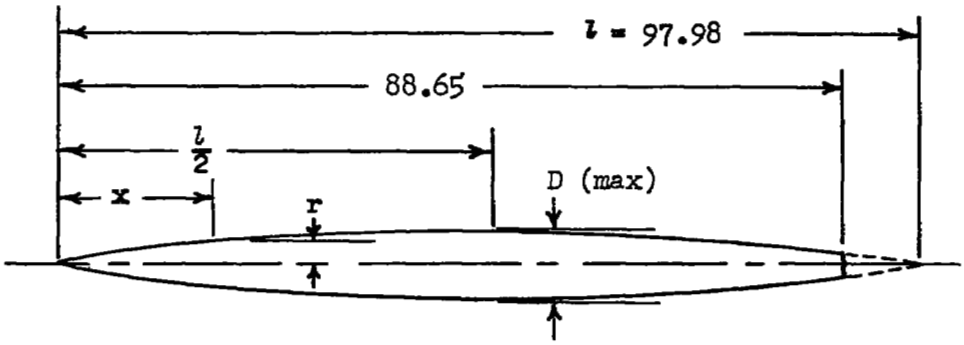

Ordinates			
x/l	r/l	x/l	r/l
0	0		
.005	.00231	0.4500	0.04143
.0075	.00298	.5000	.04167
.0125	.00428	.5500	.04130
.0250	.00722	.6000	.04024
.0500	.01205	.6500	.03842
.0750	.01613	.7000	.03562
.1000	.01971	.7500	.03128
.1500	.02593	.8000	.02526
.2000	.03090	.8333	.02083
.2500	.03465	.8500	.01852
.3000	.03741	.9000	.01125
.3500	.03933	.9500	.00439
.4000	.04063	1.0000	0.
L.E. radius: 0.0005l			

[redacted]

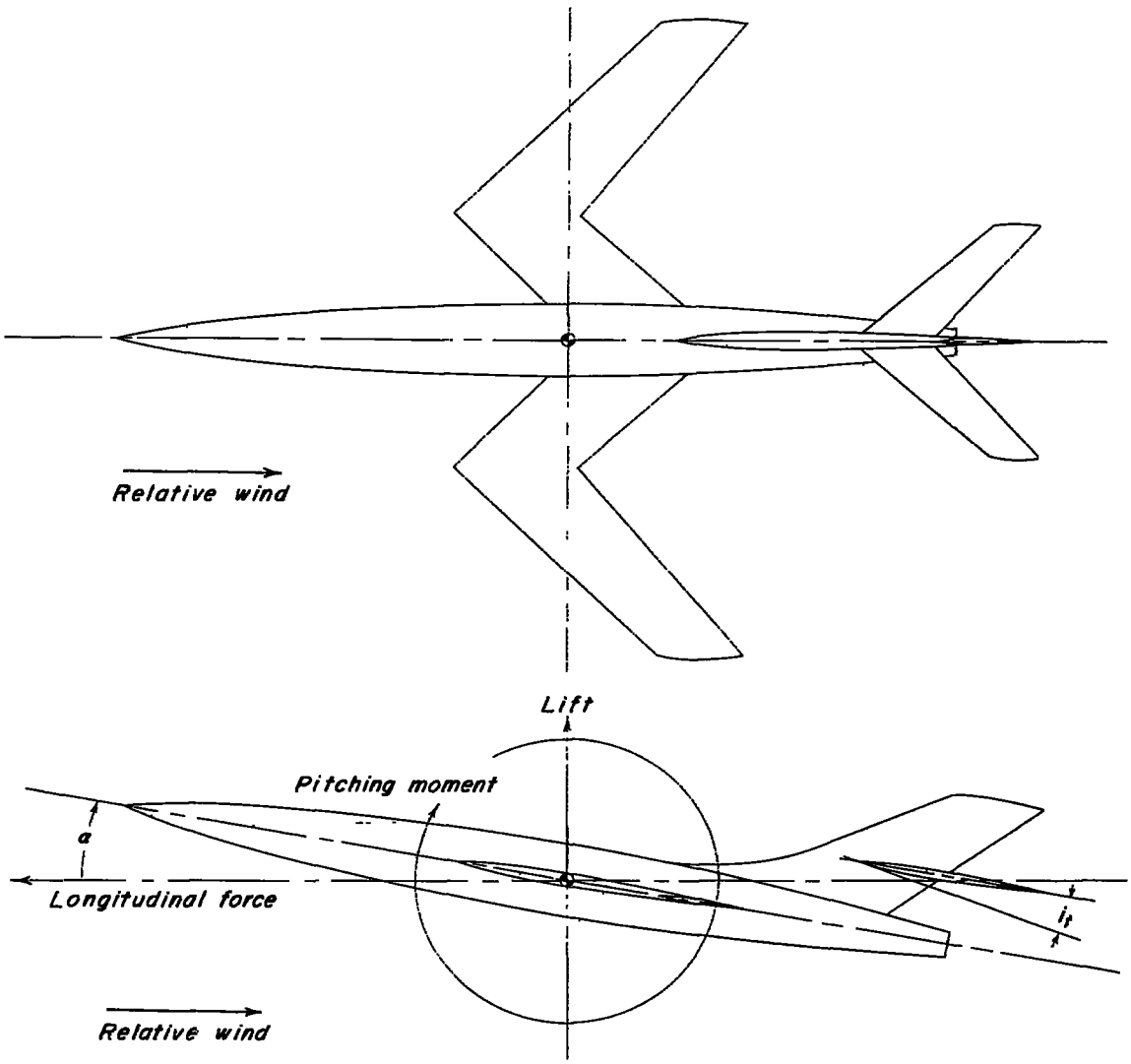

Figure 1.- Stability system of axes showing positive direction of forces, moments, and angles.

[redacted]

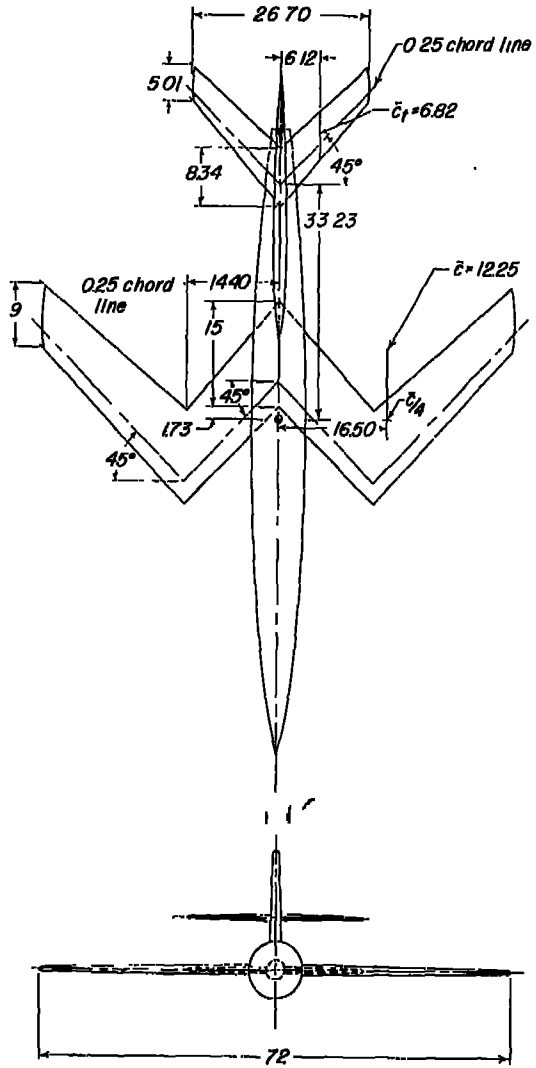

Physical Characteristics

Wing	
Sweep of $c/4$ inboard panel, deg	-45
Sweep of $c/4$ outboard panel, deg	45
Area, sq ft	6
Span, ft	6
Aspect ratio	6
Taper ratio	0.60
Mean aerodynamic chord, ft	1.02
Incidence, deg	0
Dihedral, deg	0
Airfoil section parallel to plane of symmetry	65A009
Horizontal tail	
Area, sq ft	1.24
Aspect ratio	4.00
Airfoil section parallel to plane of symmetry	NACA 65A006
Vertical tail	
Area, sq ft	1.69
Aspect ratio	1.18
Airfoil section parallel to plane of symmetry	63A009

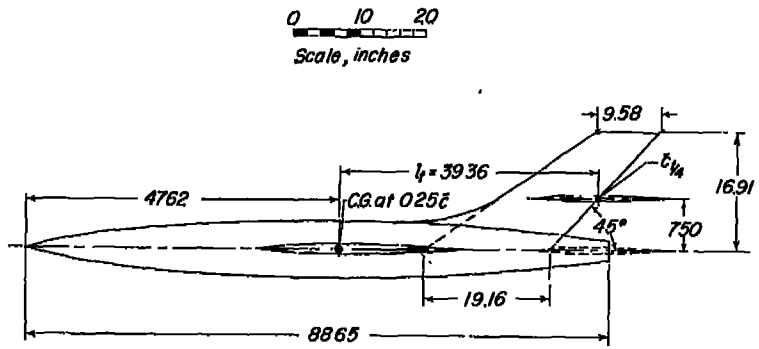

Figure 2.- General arrangement of test model with typical M-wing.

L-68568

Figure 3.- Photograph of typical model on support strut.

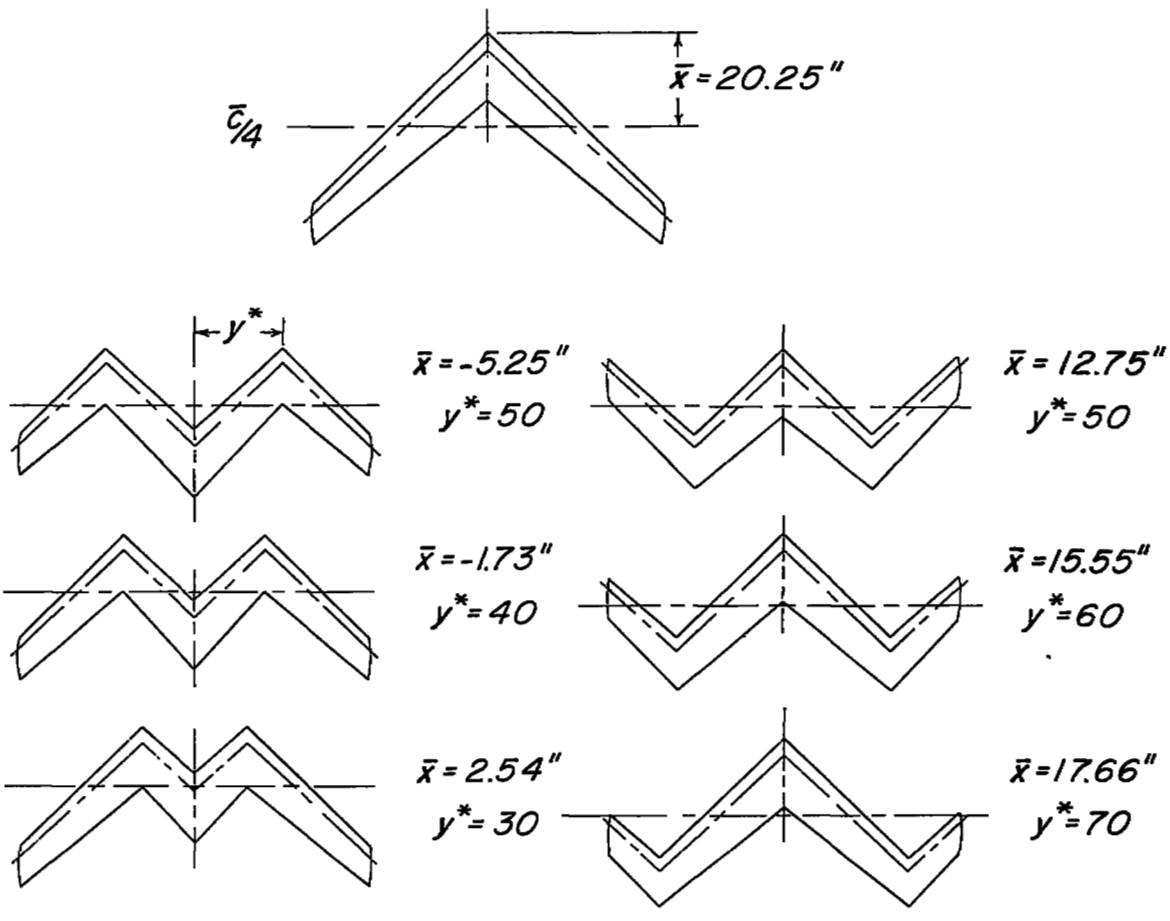

Aspect ratio	6.0
Taper ratio	.6
Sweep of $c/4$, deg	± 45
Span, ft	6
Area, sq ft	6
Mean aerodynamic chord, ft	1.02
Airfoil section parallel to plane of symmetry	NACA 65A009

Figure 4.- Details of the various M- and W-wings.

[redacted]

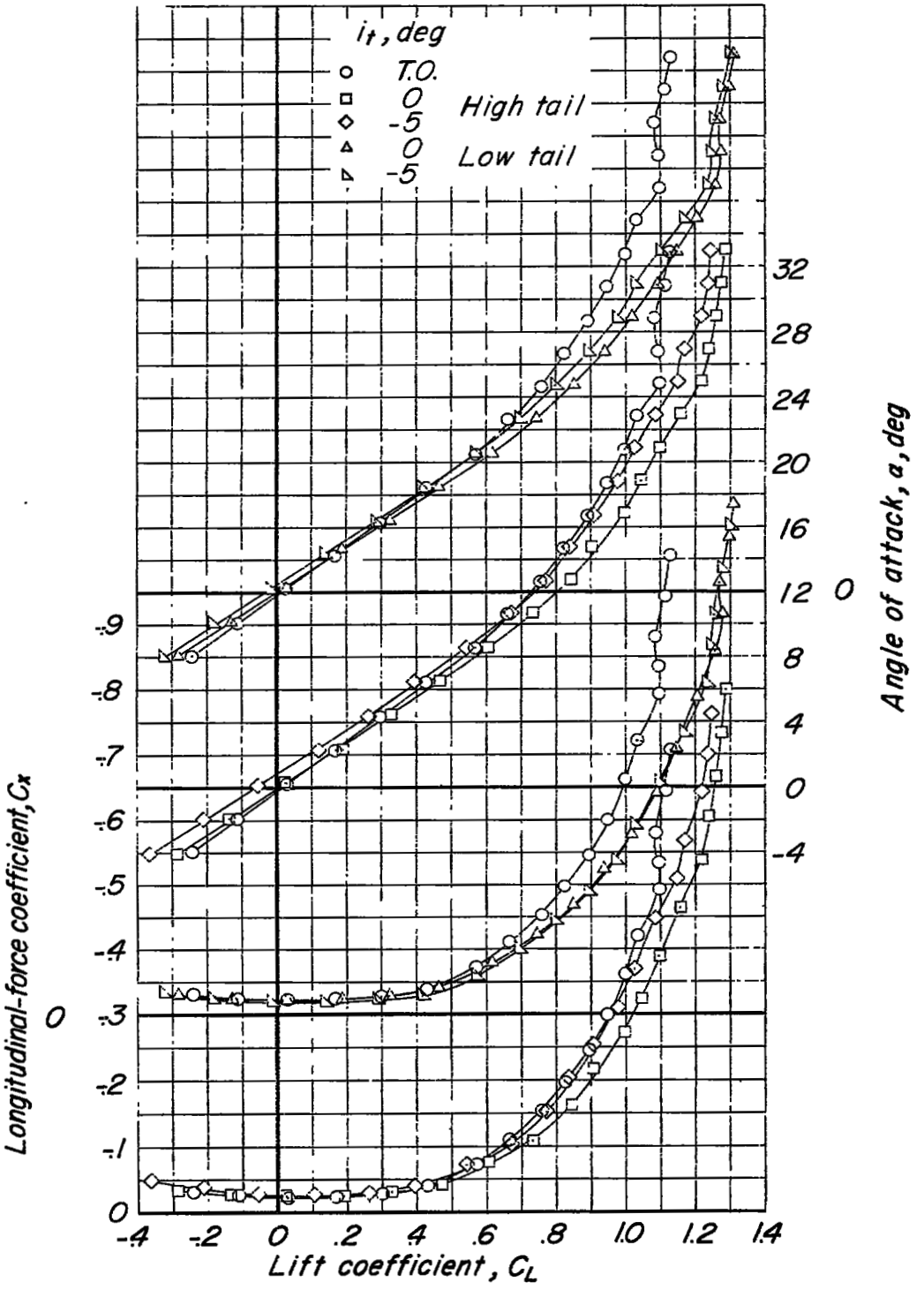

Figure 5.- Effect of horizontal-tail incidence and height on aerodynamic characteristics of model with a 45° swept wing.

[redacted]

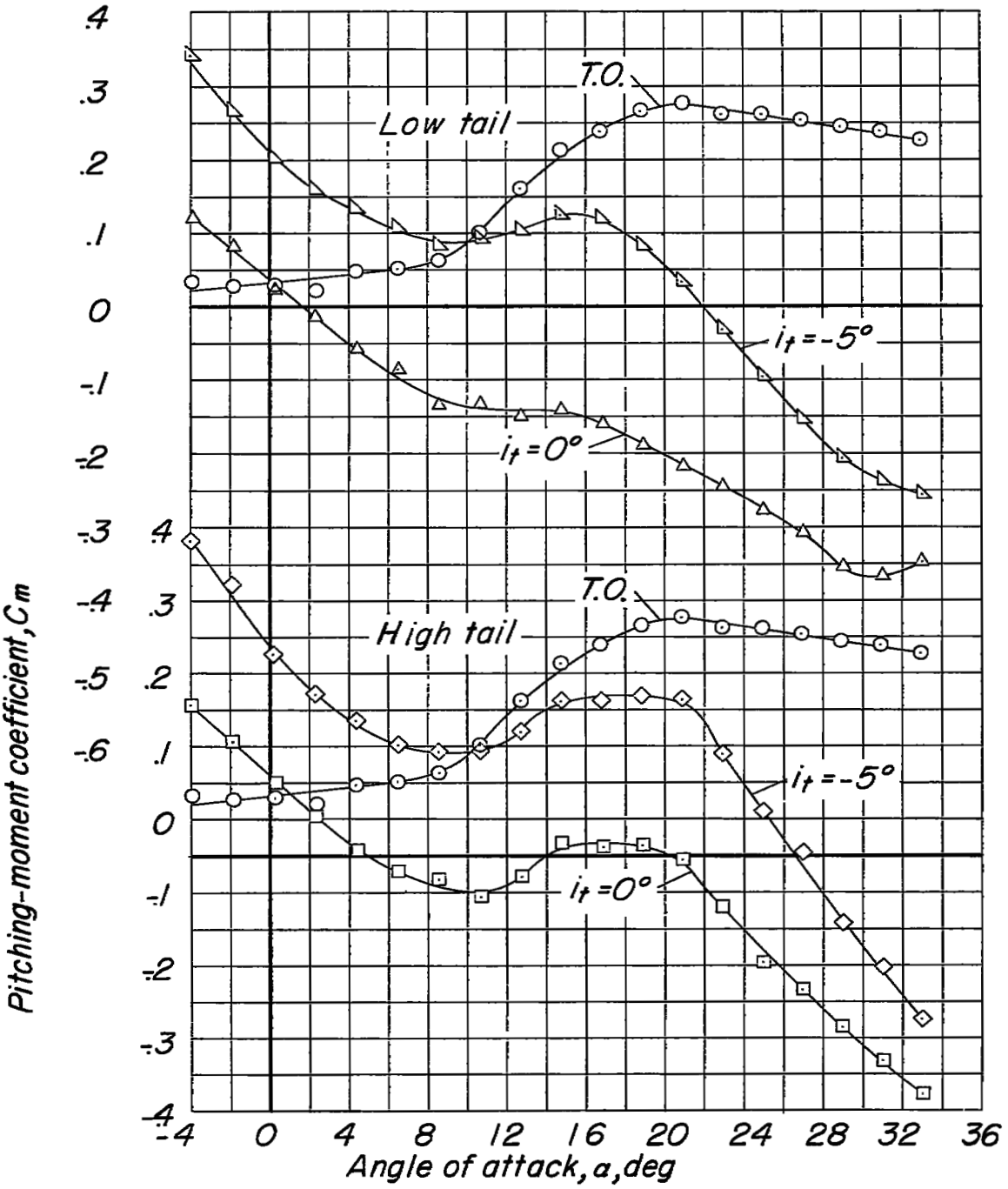

Figure 5.- Concluded.

[redacted]

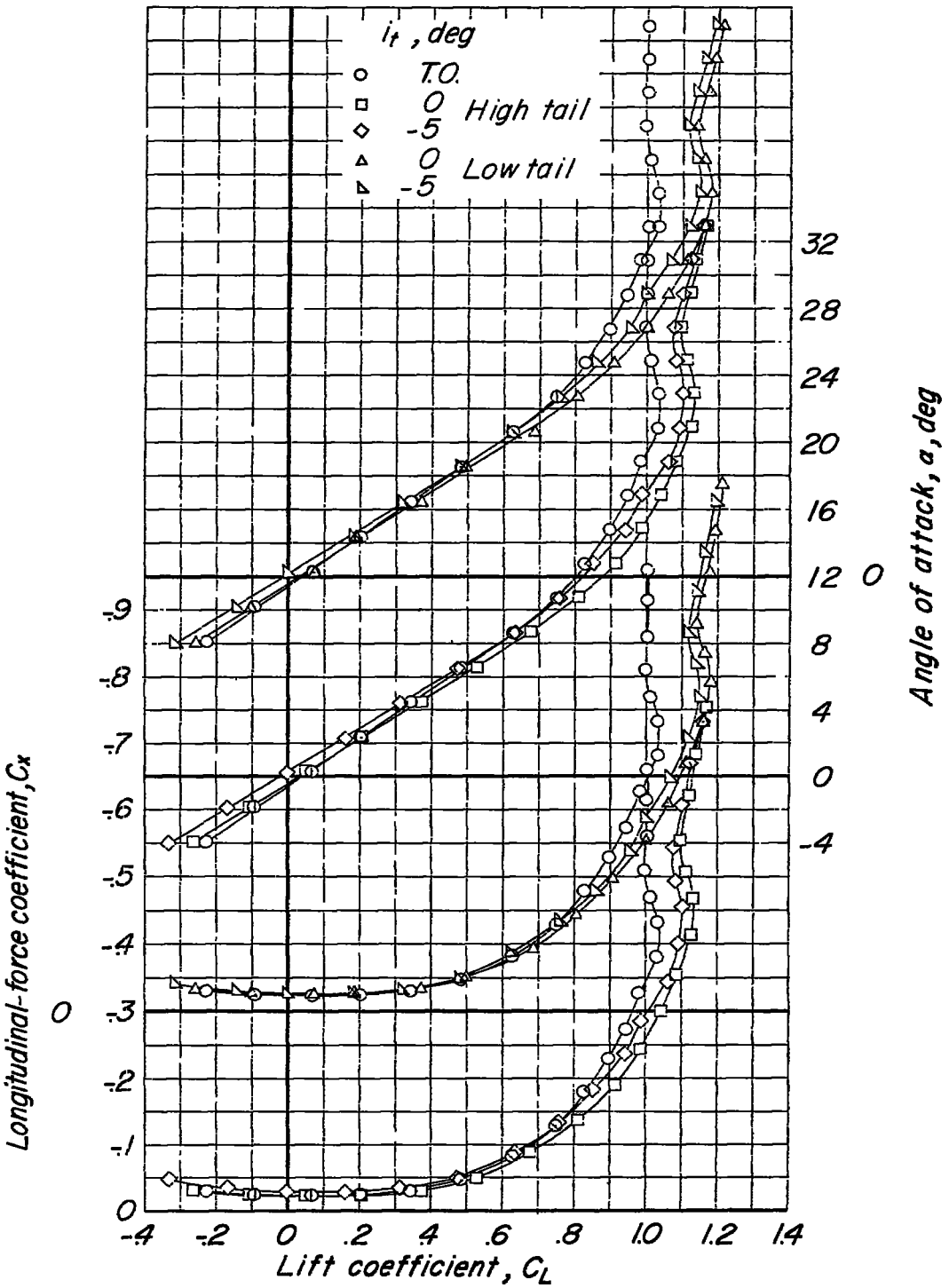

Figure 6.- Effect of horizontal-tail incidence and height on aerodynamic characteristics of model with M-wing having y^* = 30 percent b/2.

[redacted]

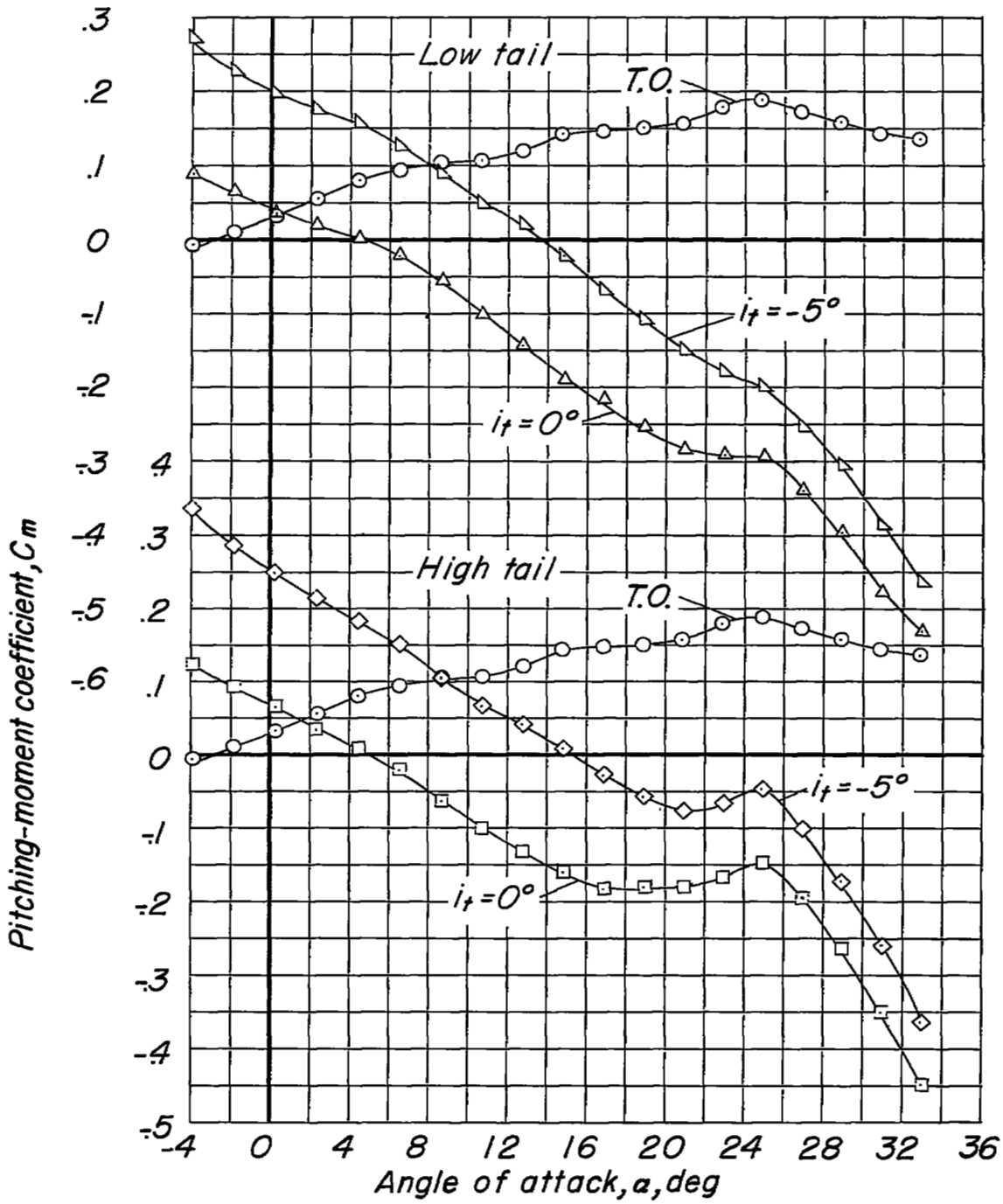

Figure 6.- Concluded.

[redacted]

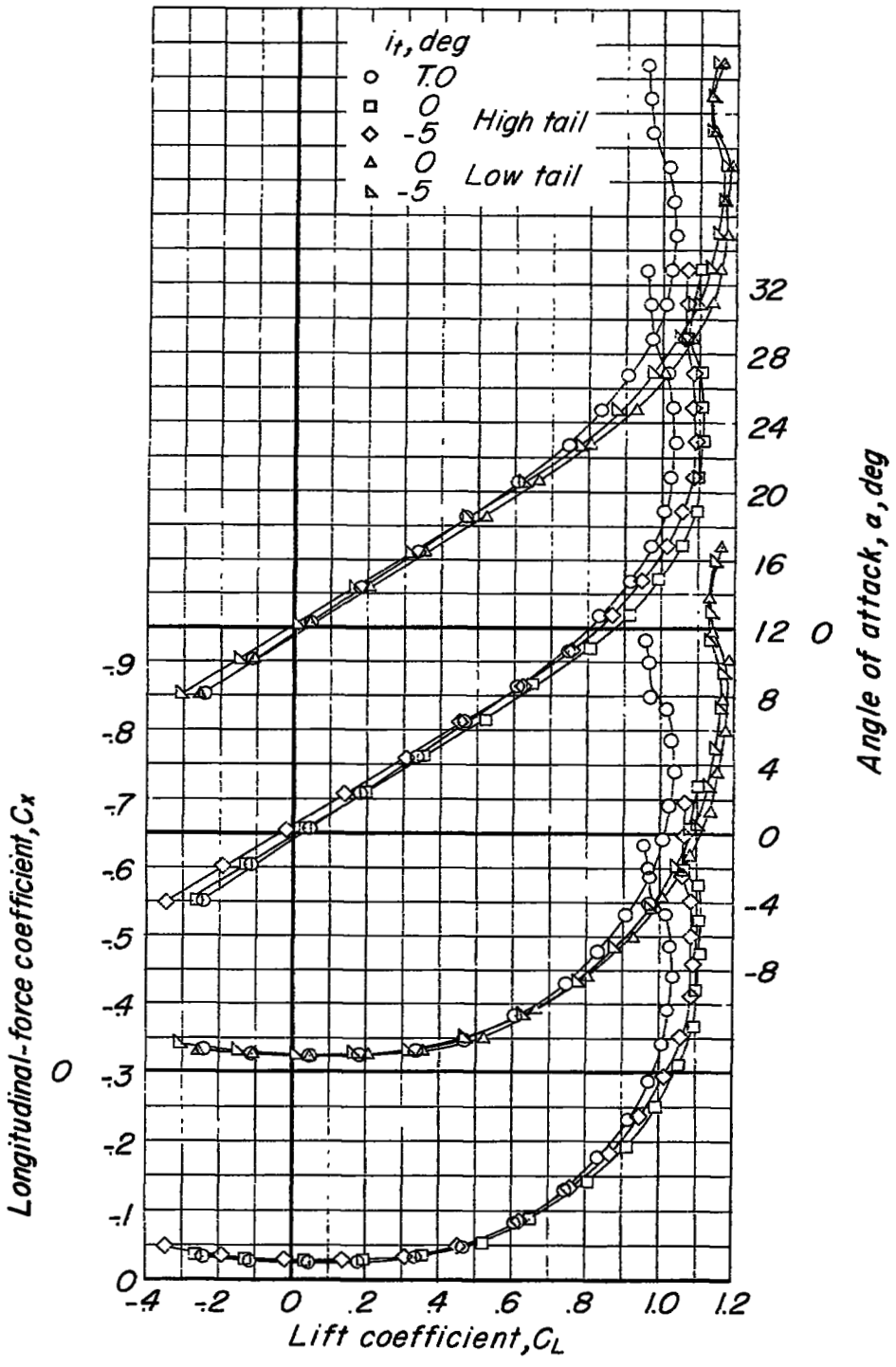

Figure 7.- Effect of horizontal-tail incidence and height on aerodynamic characteristics of the model with M-wing having y* = 40 percent b/2.

[redacted]

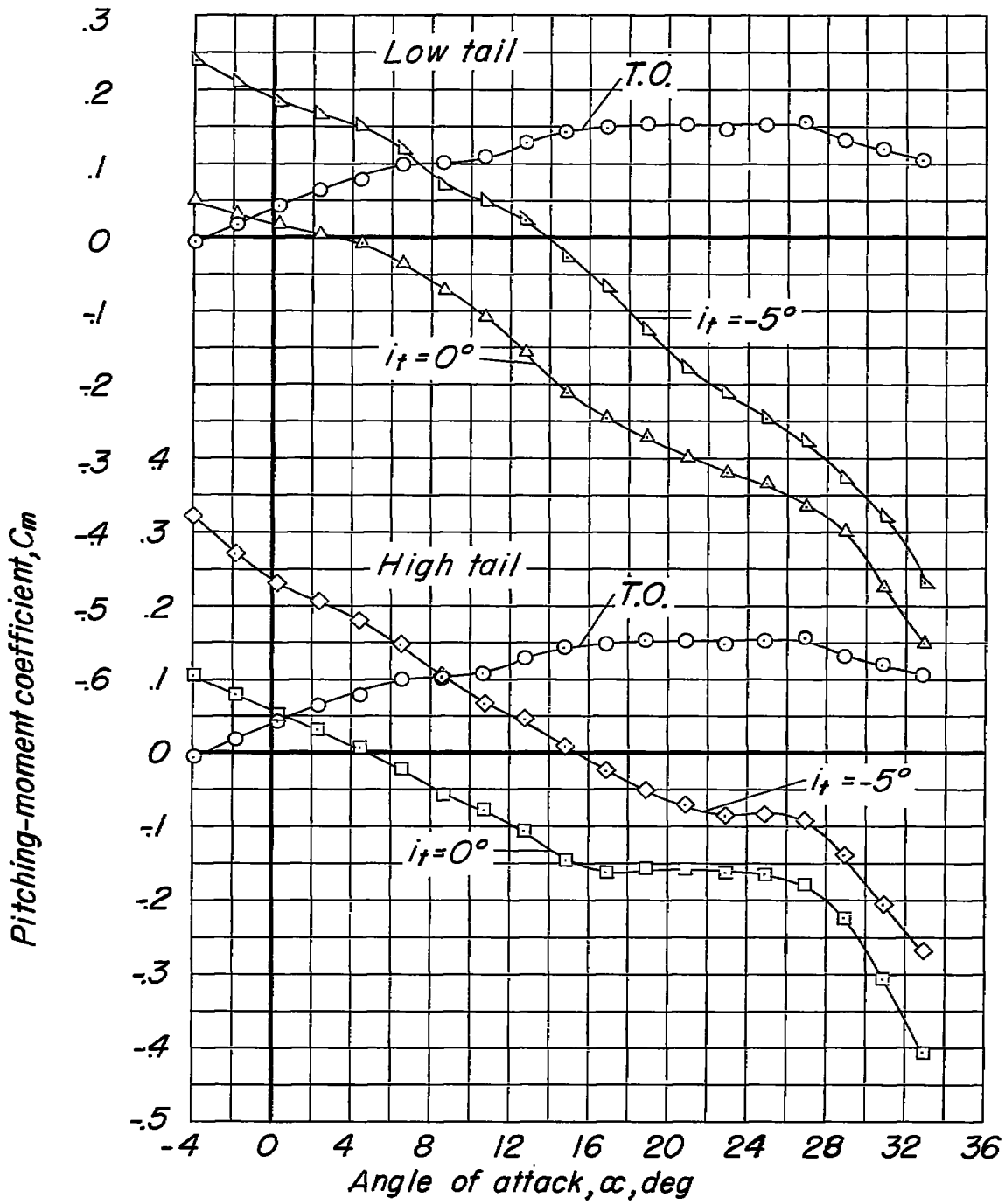

Figure 7.- Concluded.

[redacted]

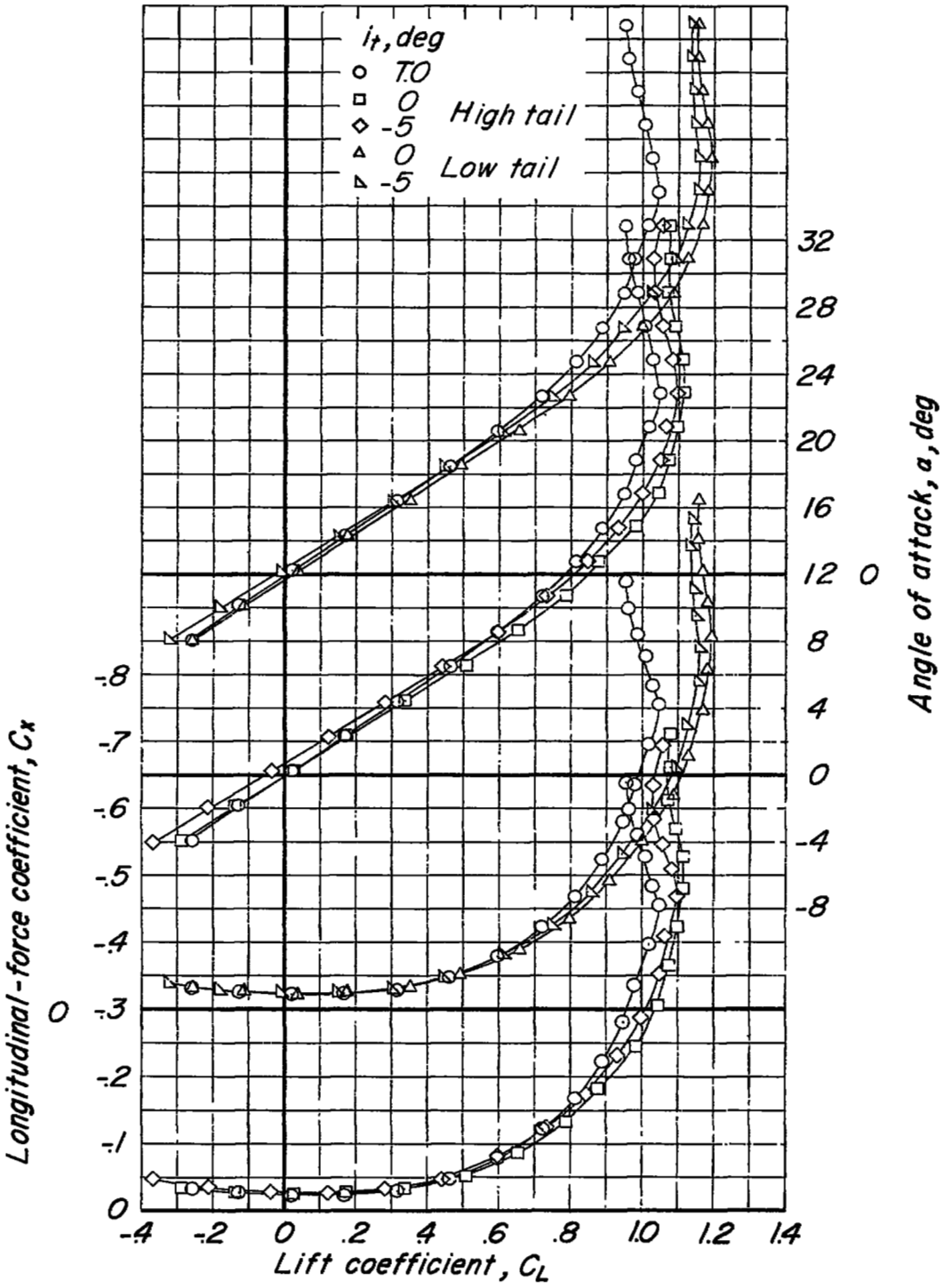

Figure 8.- Effect of horizontal-tail incidence and height on aerodynamic characteristics of model with M-wing having y* = 50 percent b/2.

[redacted]

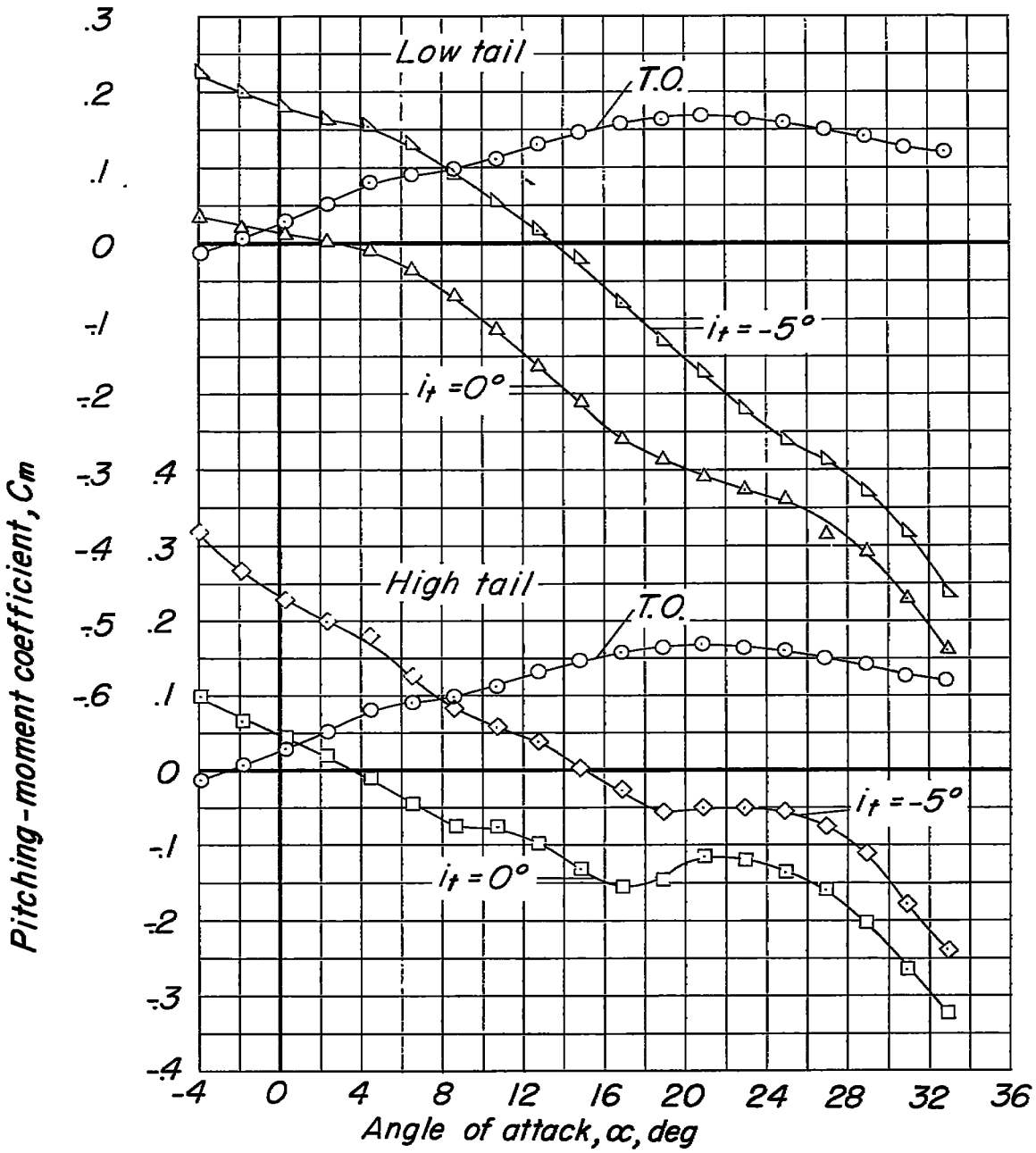

Figure 8.- Concluded.

[redacted]

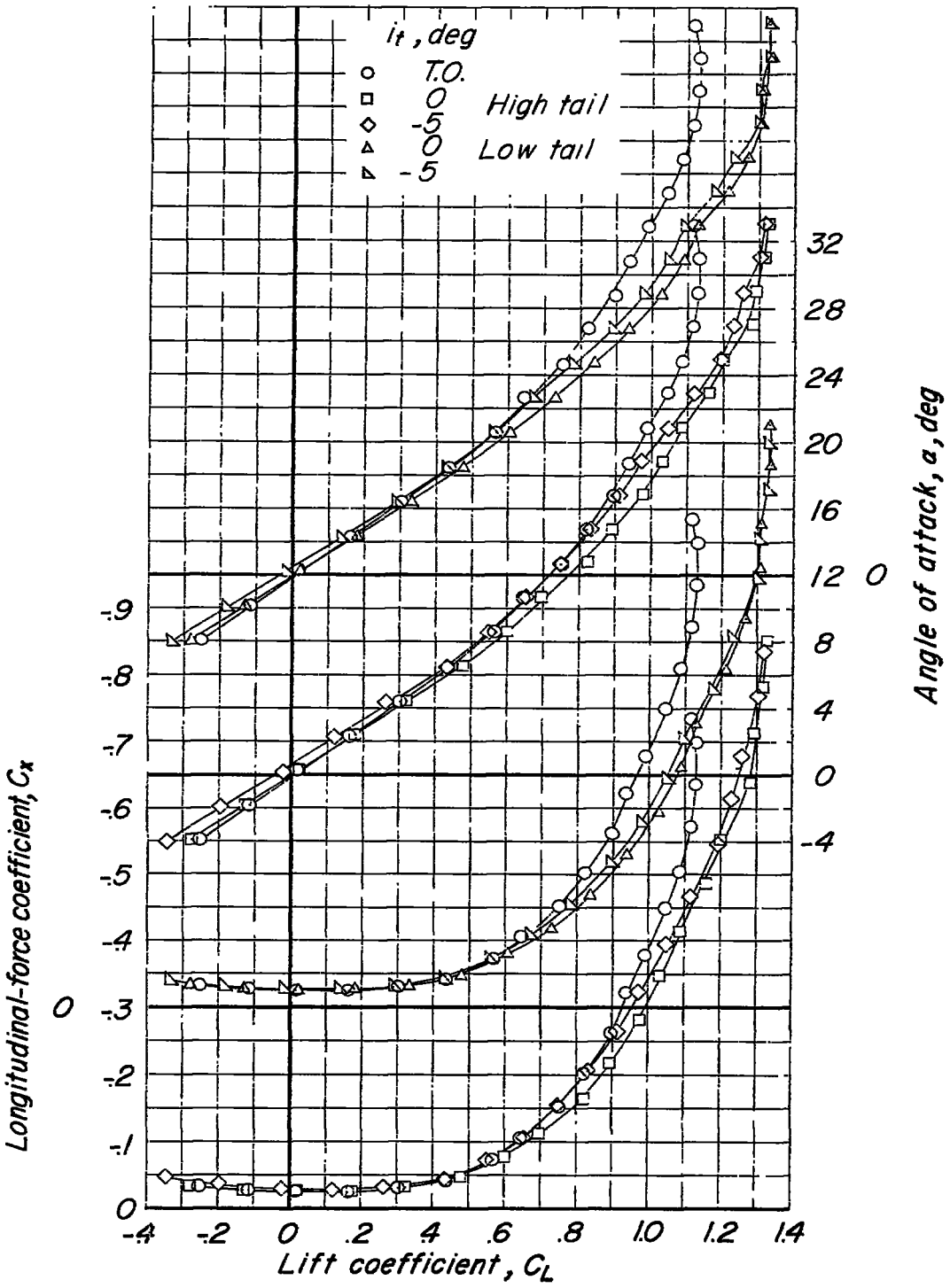

Figure 9.- Effect of horizontal-tail incidence and height on aerodynamic characteristics of model with W-wing having y* = 50 percent b/2.

[redacted]

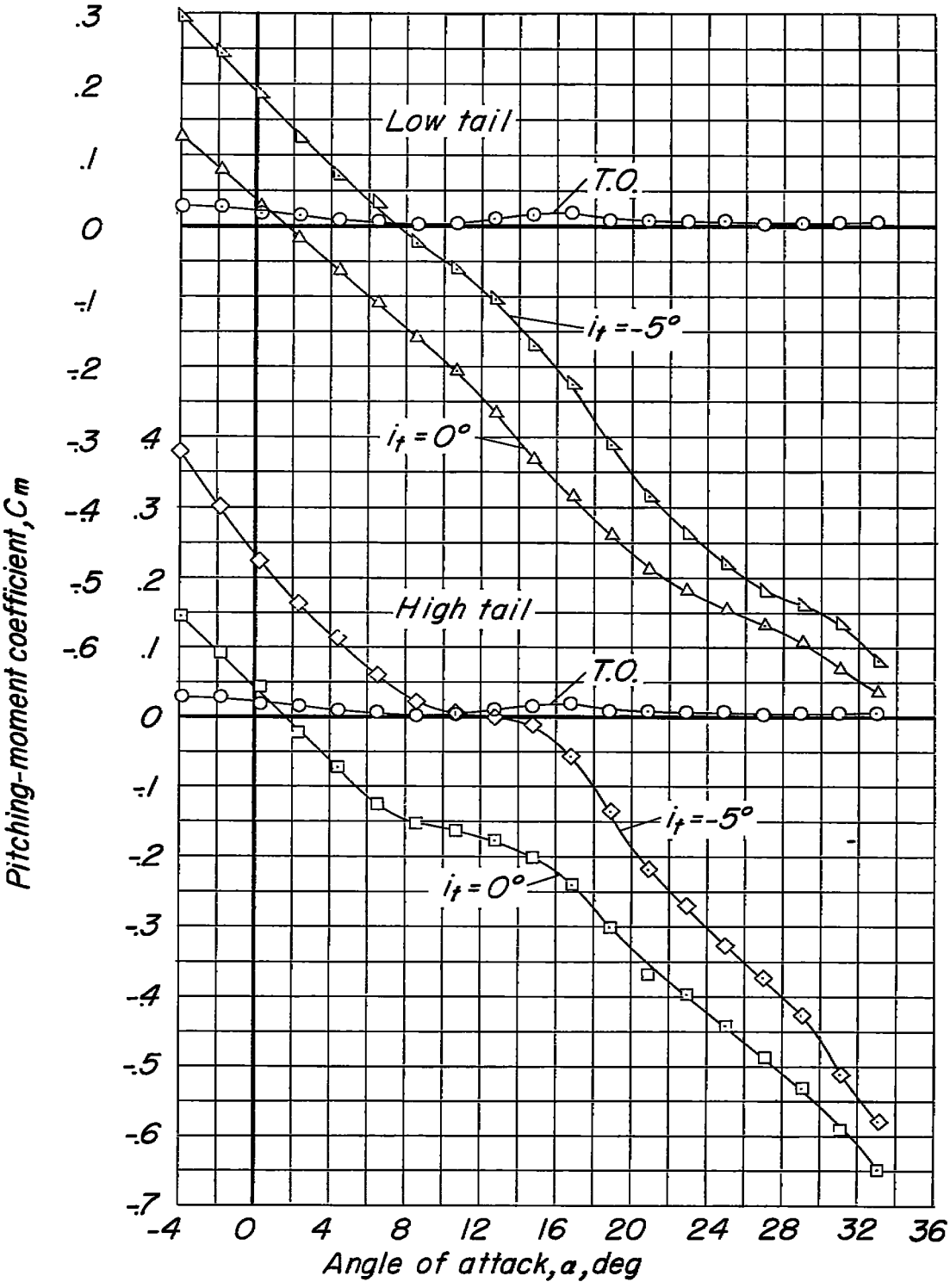

Figure 9.- Concluded.

[redacted]

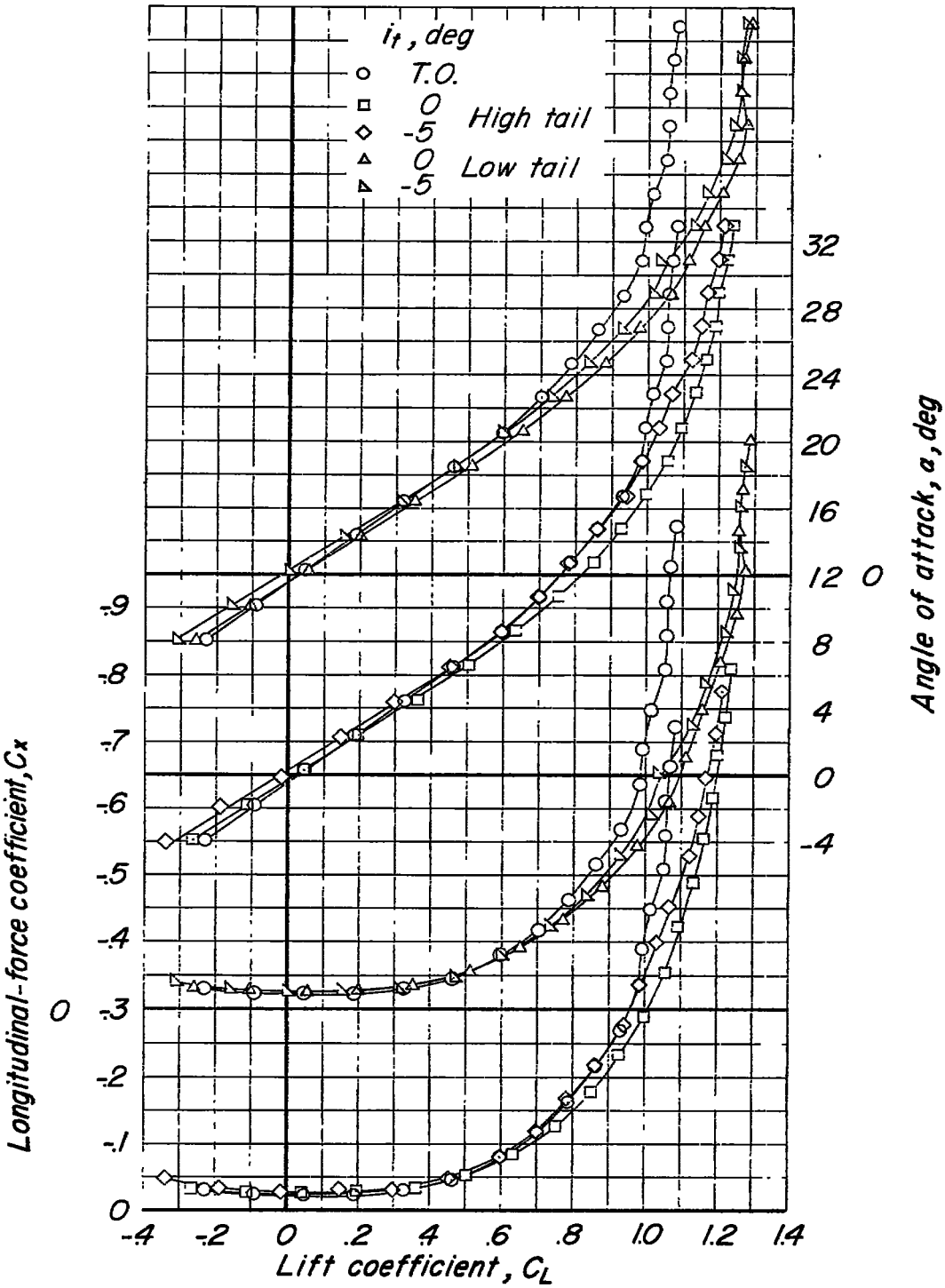

Figure 10.- Effect of horizontal-tail incidence and height on aerodynamic characteristics of model with W-wing having $y^* = 60$ percent b/2.

[redacted]

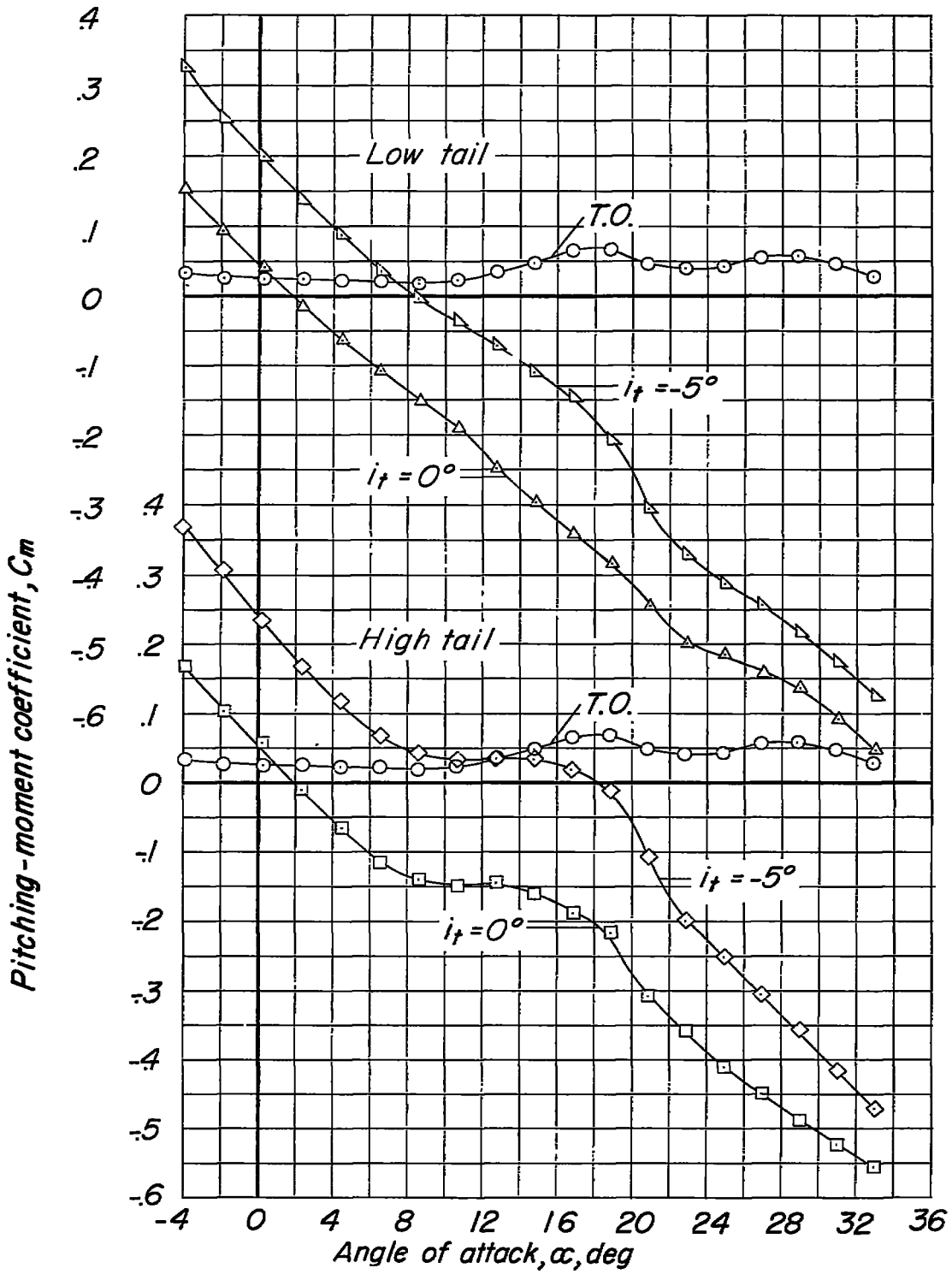

Figure 10.- Concluded.

[redacted]

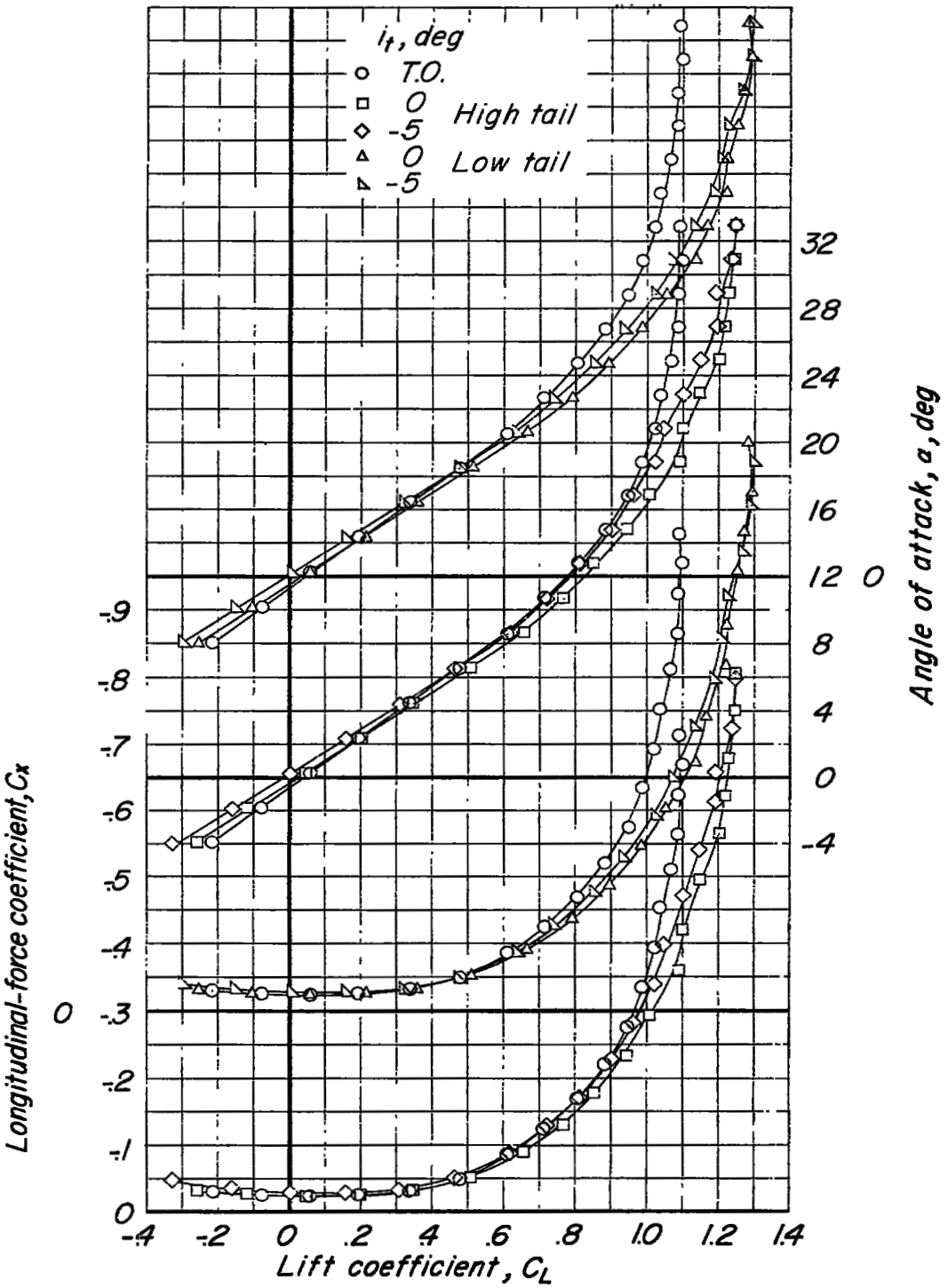

Figure 11.- Effect of horizontal-tail incidence and height on aerodynamic characteristics of model with W-wing having $y^* = 70$ percent $b/2$.

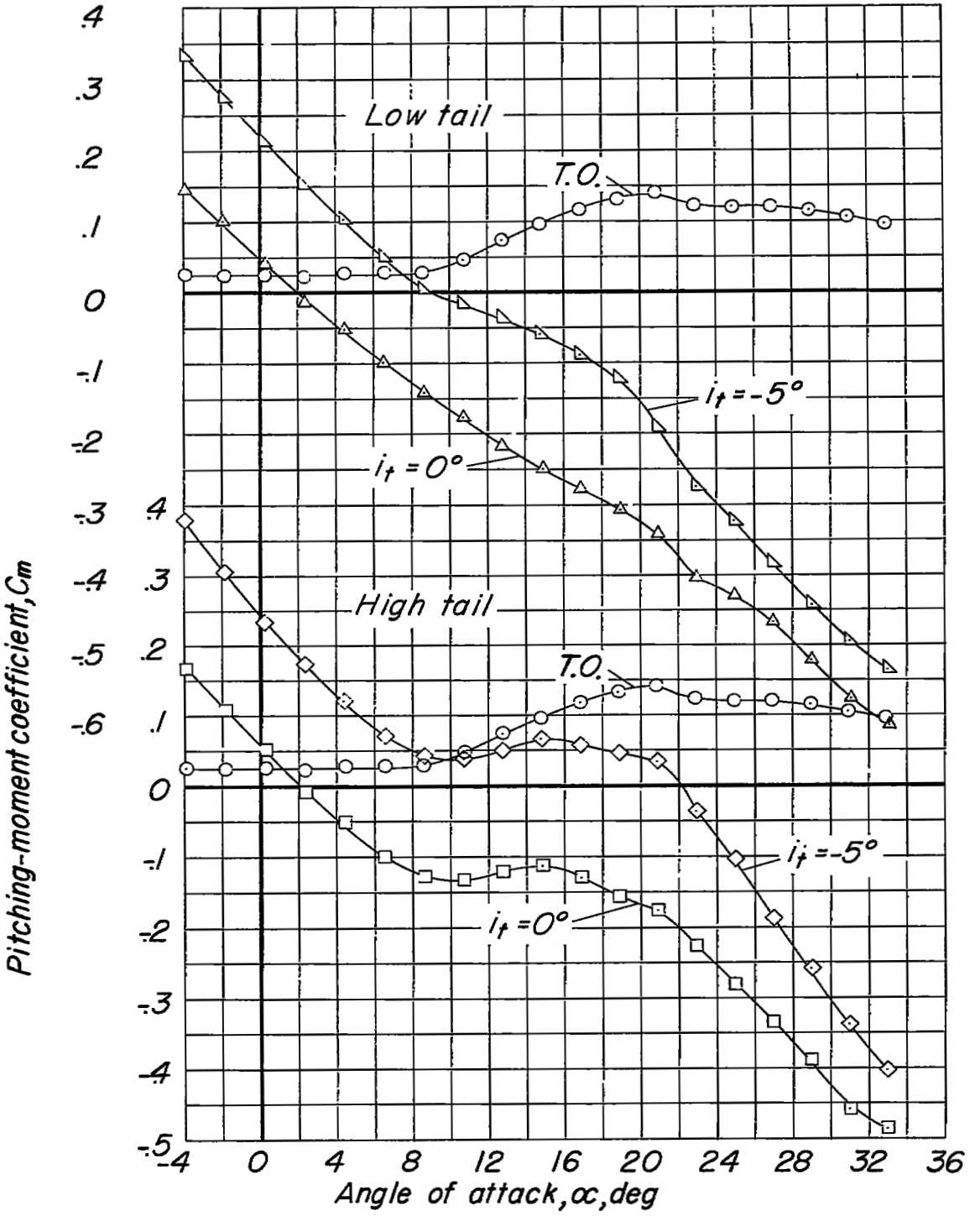

Figure 11.- Concluded.

[redacted]

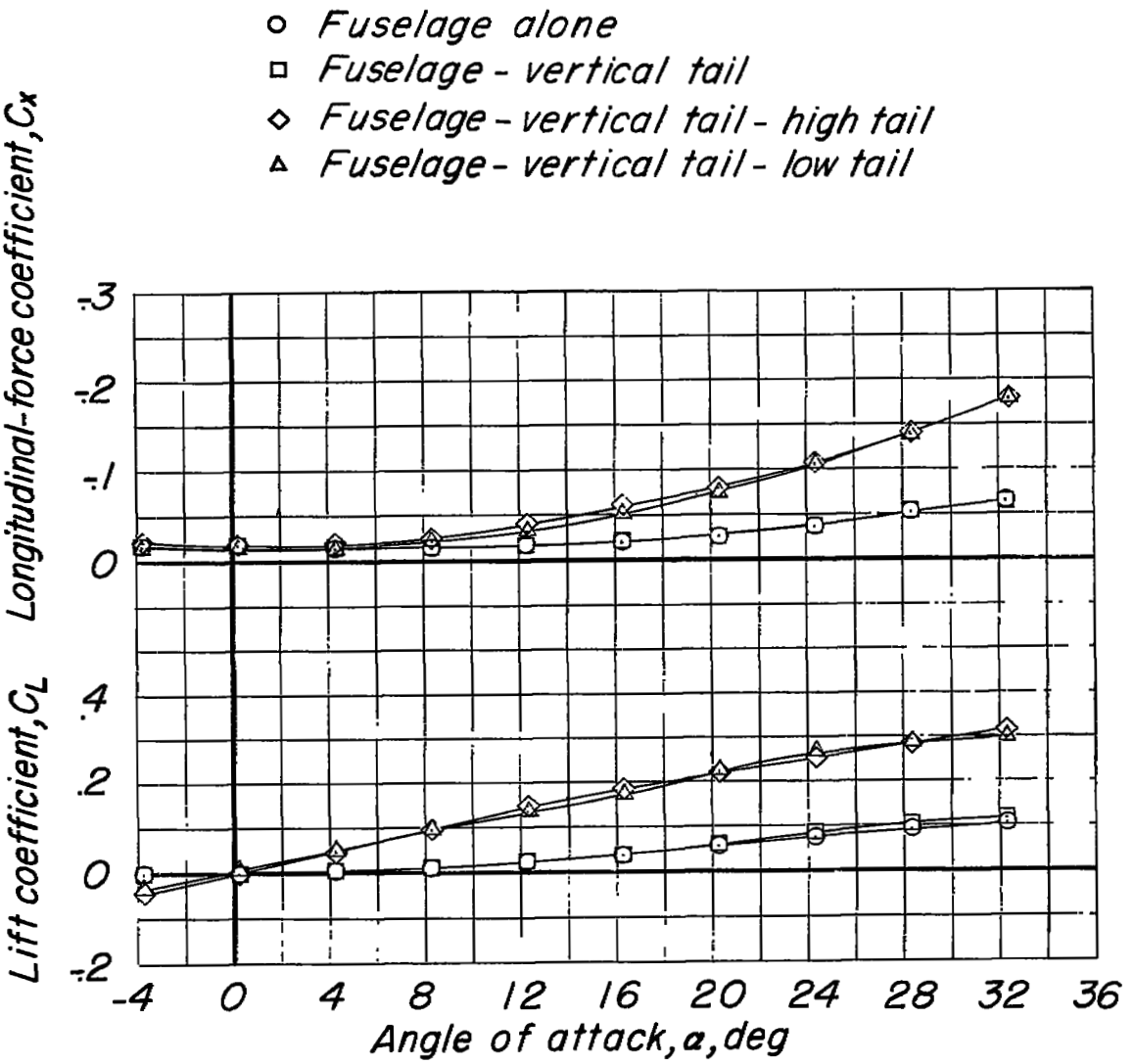

Figure 12.- Effect of angle of attack on aerodynamic characteristics of model without a wing.

[redacted]

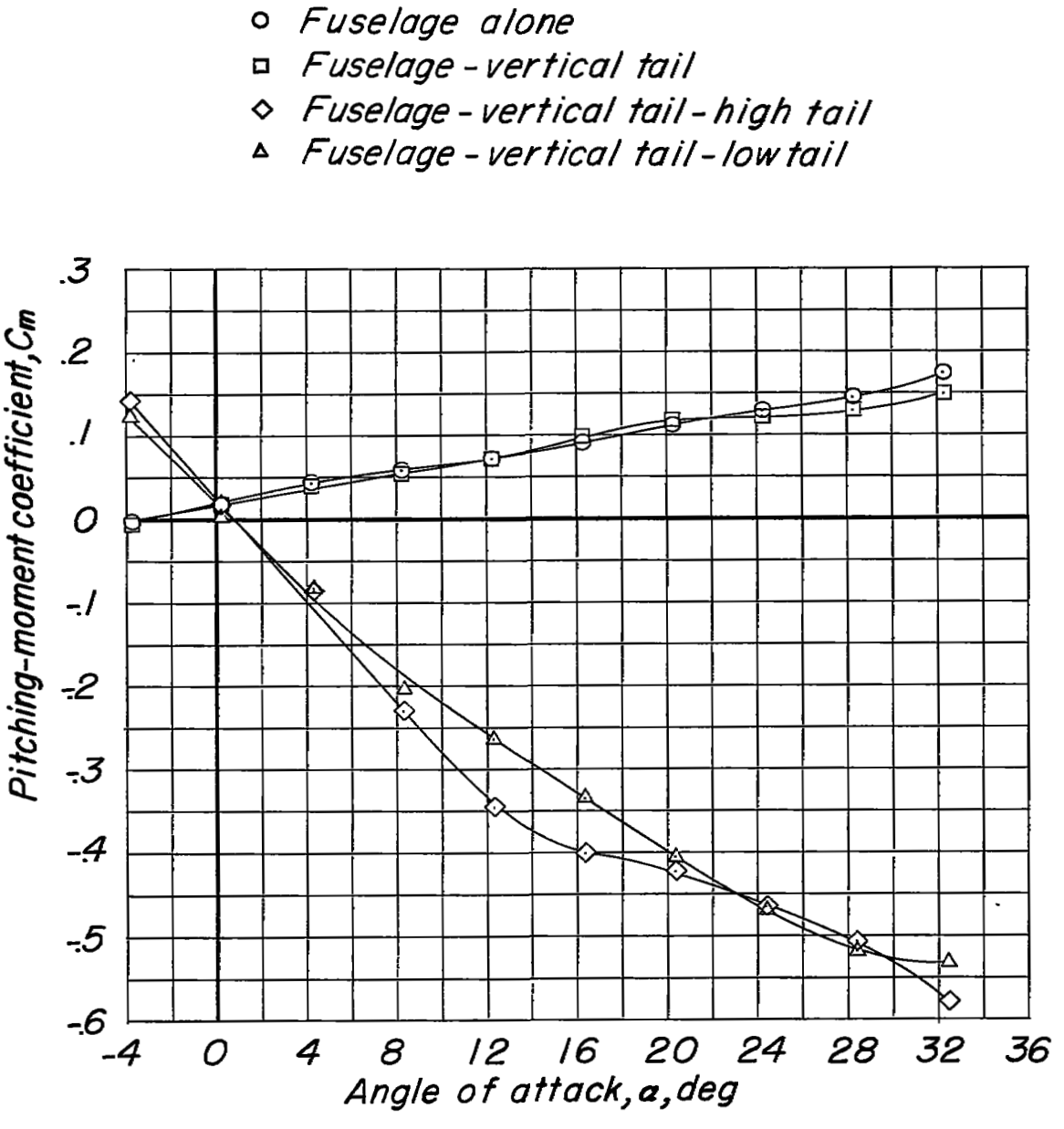

Figure 12.- Concluded.

[redacted]

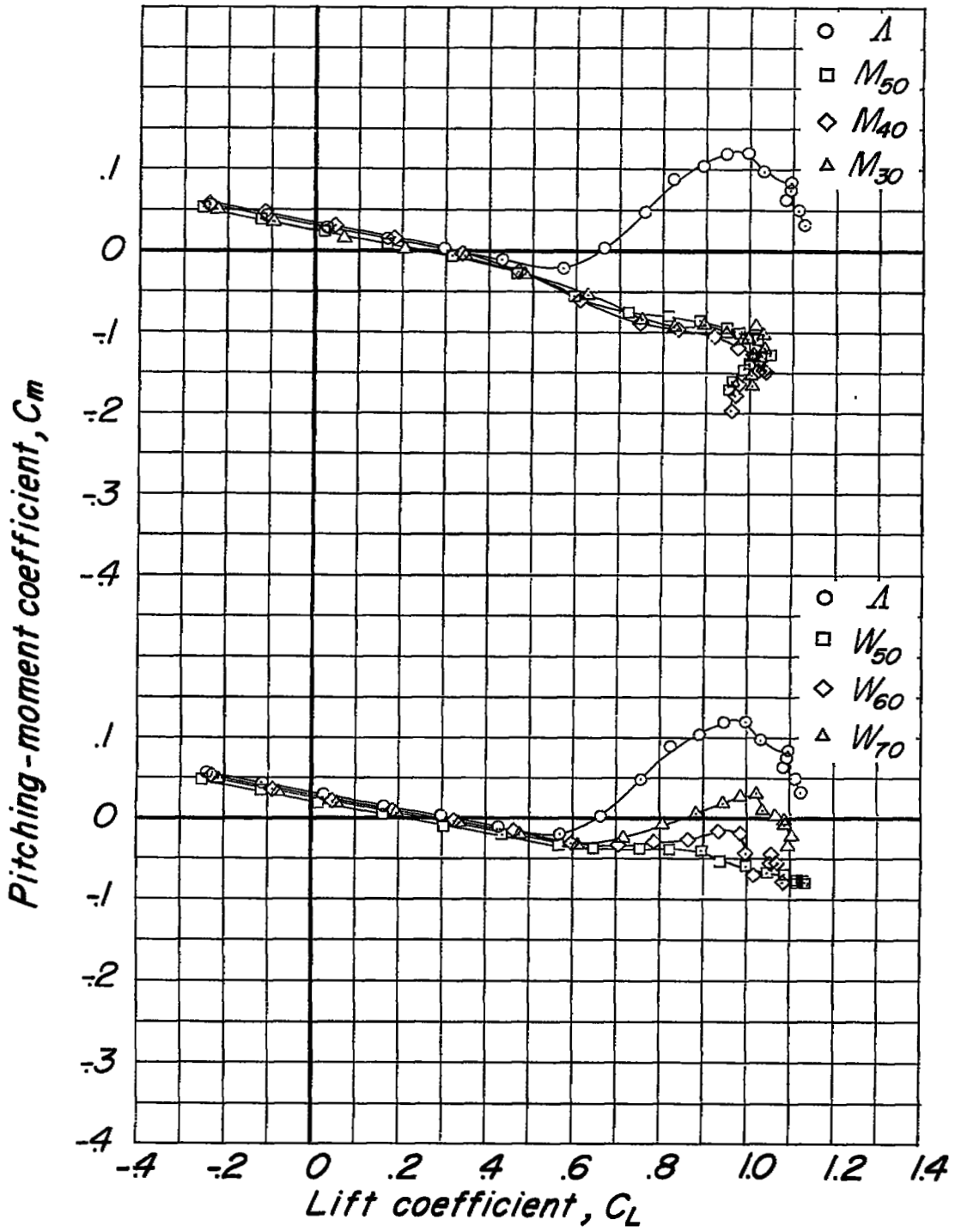

(a) Horizontal tail off.

Figure 13.- Longitudinal stability characteristics of test model with various wings. Static margin adjusted to 0.10$\bar{c}$.

[redacted]

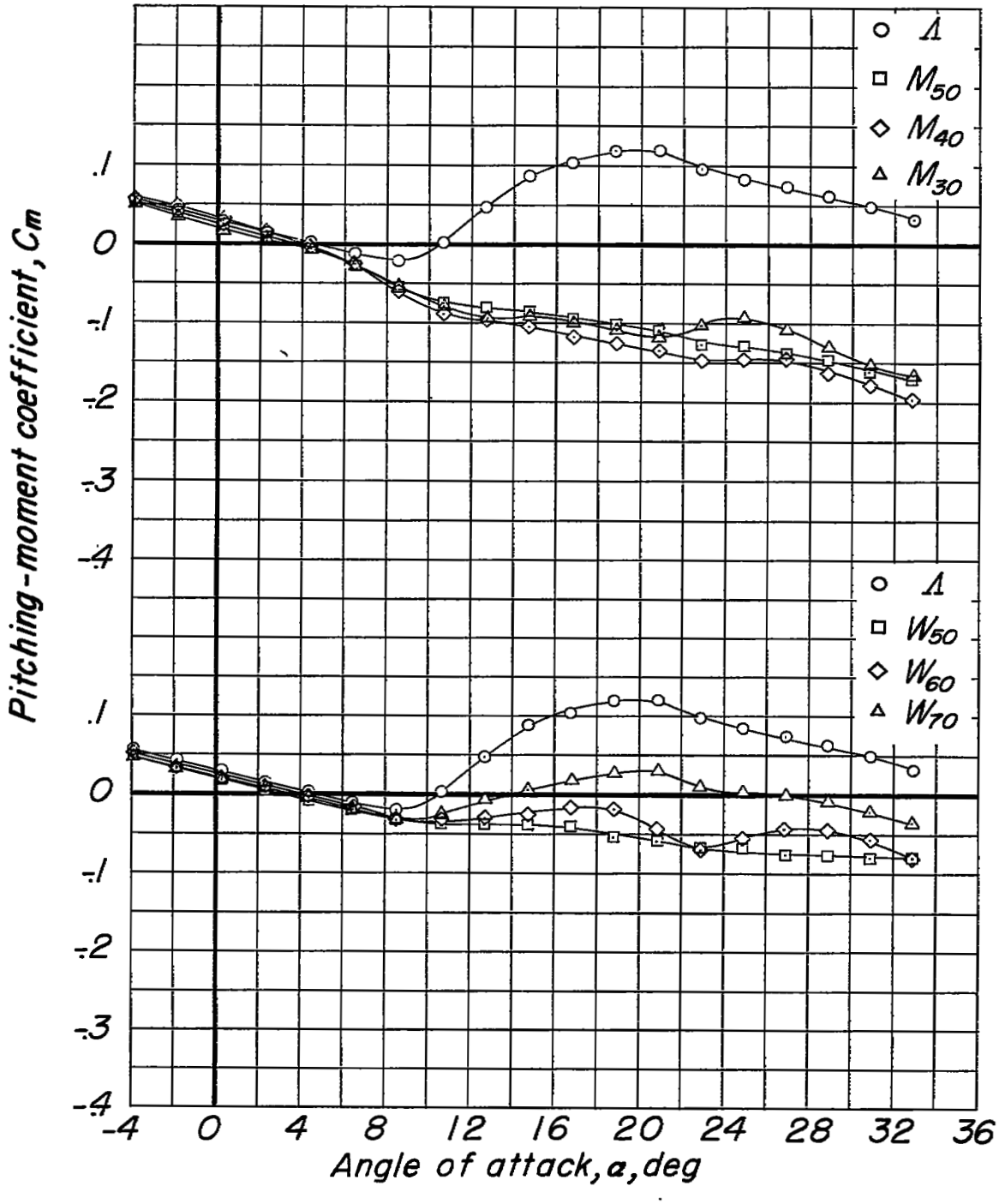

(a) Concluded. (Tail off.)

Figure 13.- Continued.

[redacted]

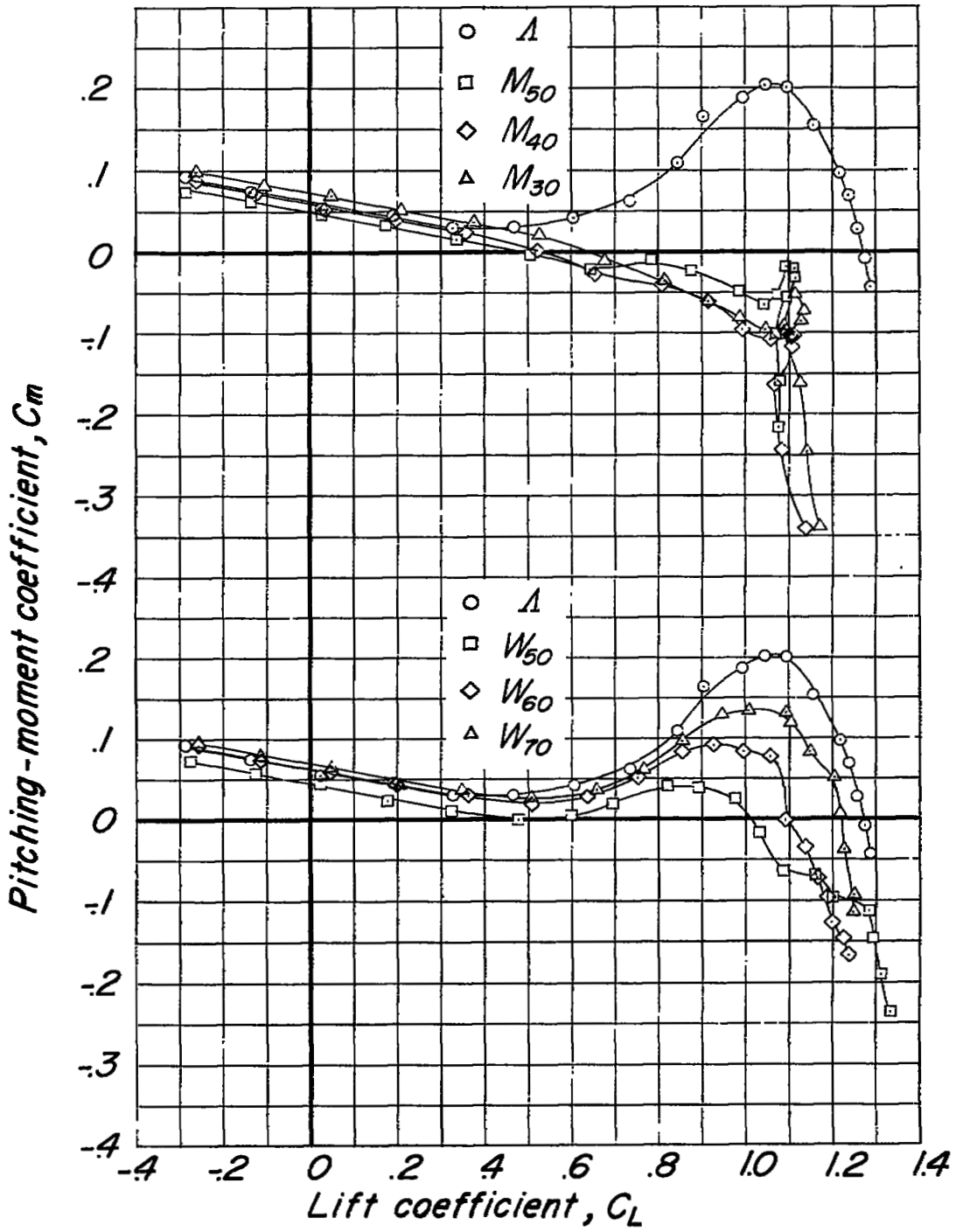

(b) High tail.

Figure 13.- Continued.

[redacted]

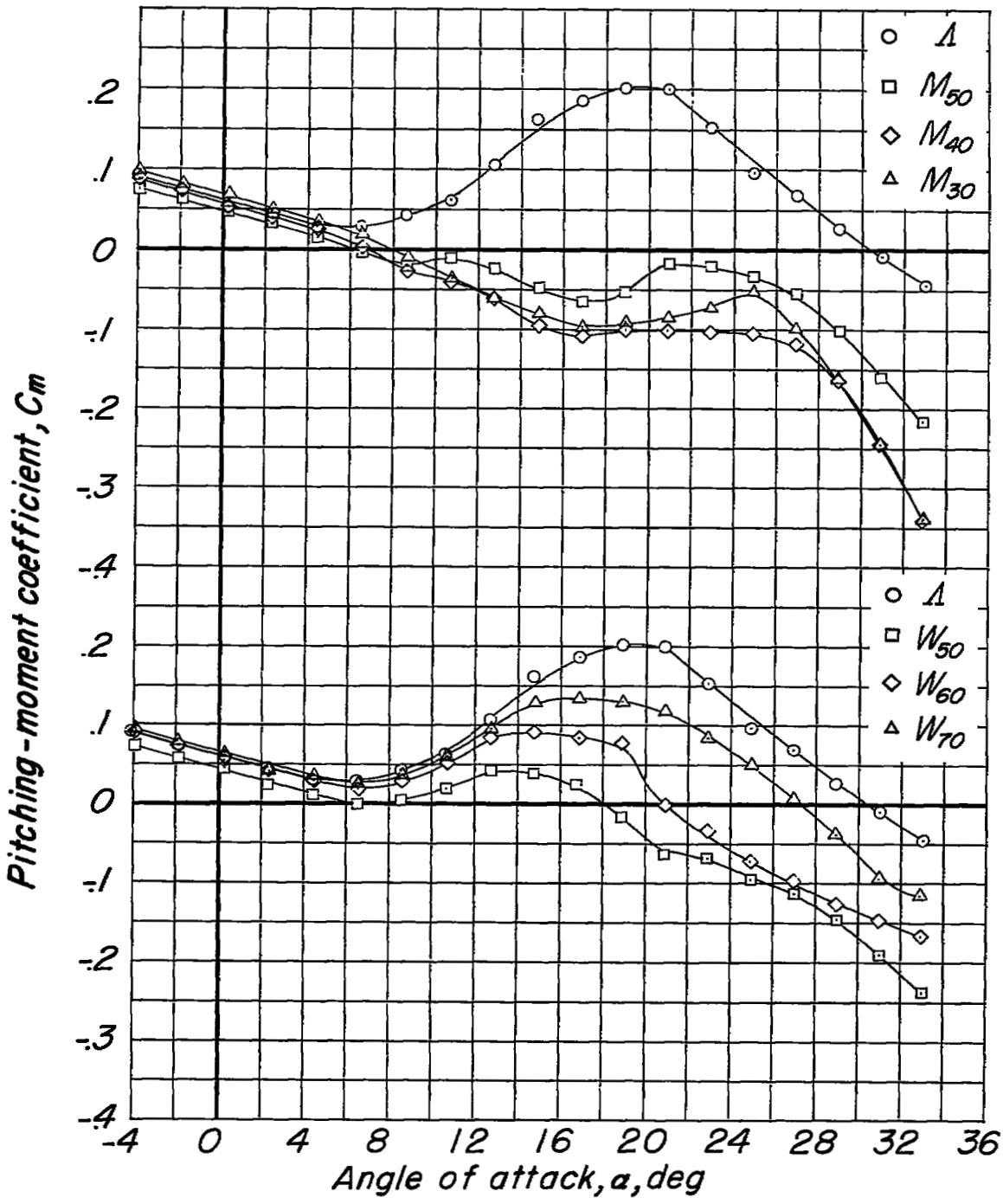

(b) Concluded. (High tail.)

Figure 13.- Continued.

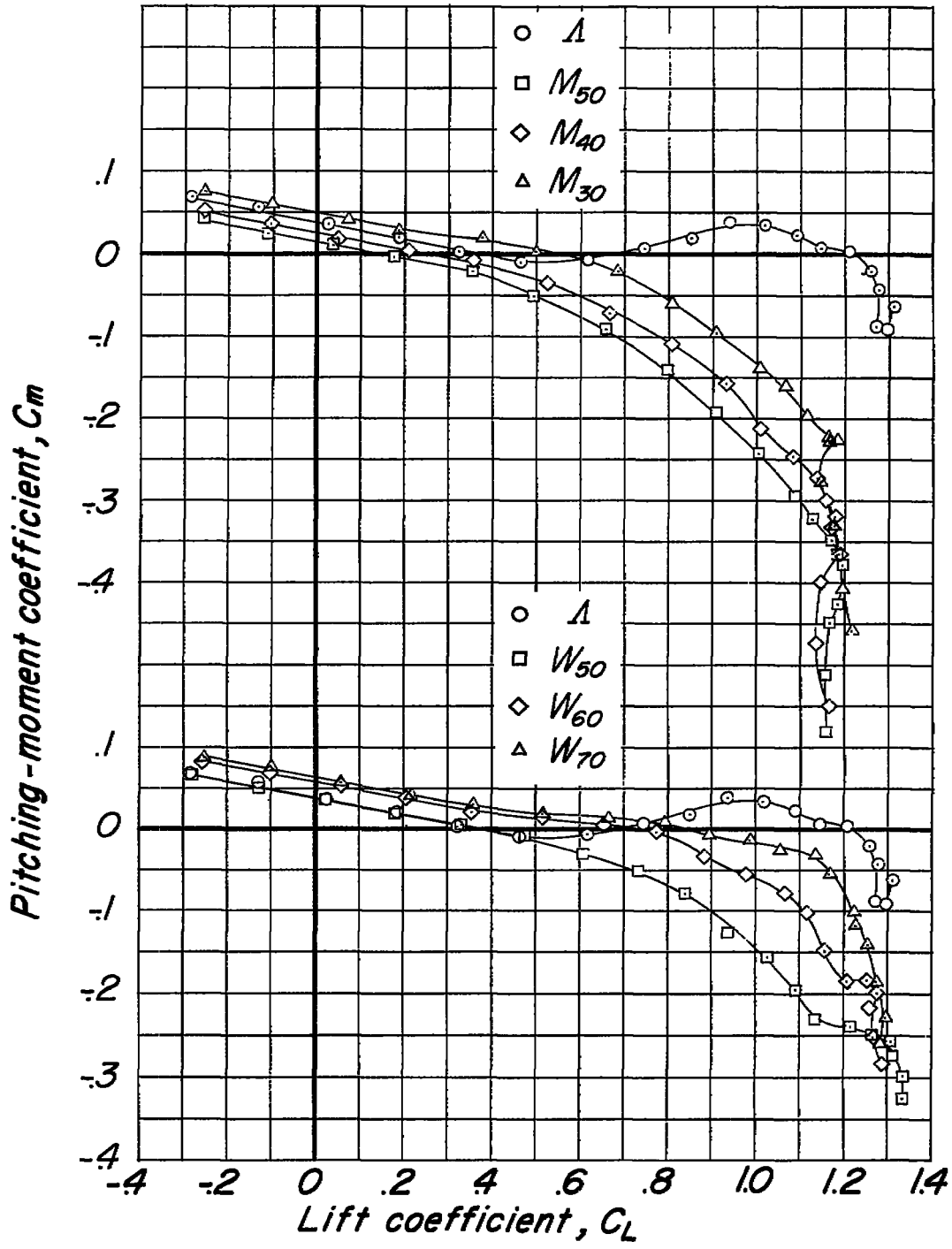

(c) Low tail.

Figure 13.- Continued.

[redacted]

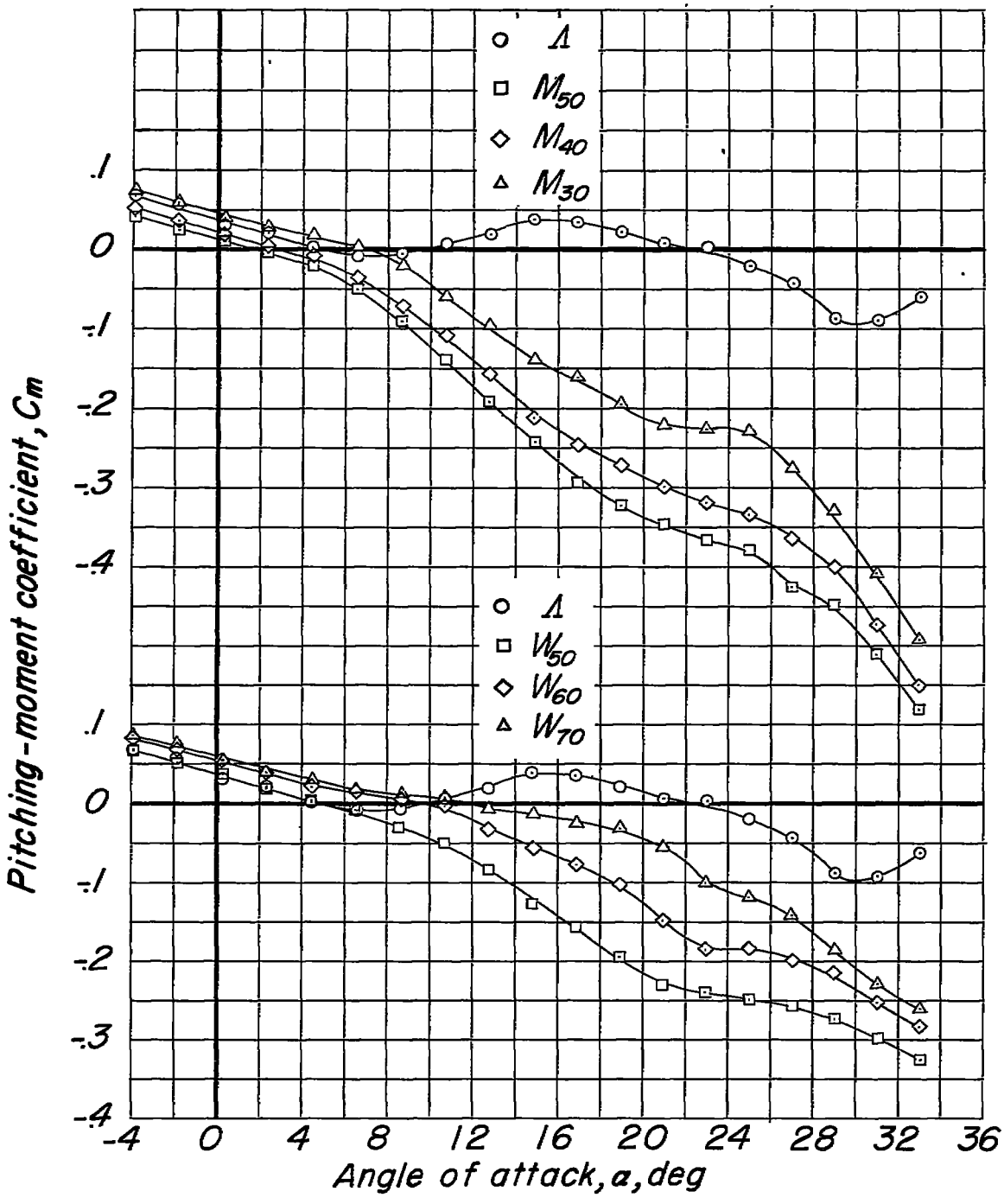

(c) Concluded. (Low tail.)

Figure 13.- Concluded.

[redacted]

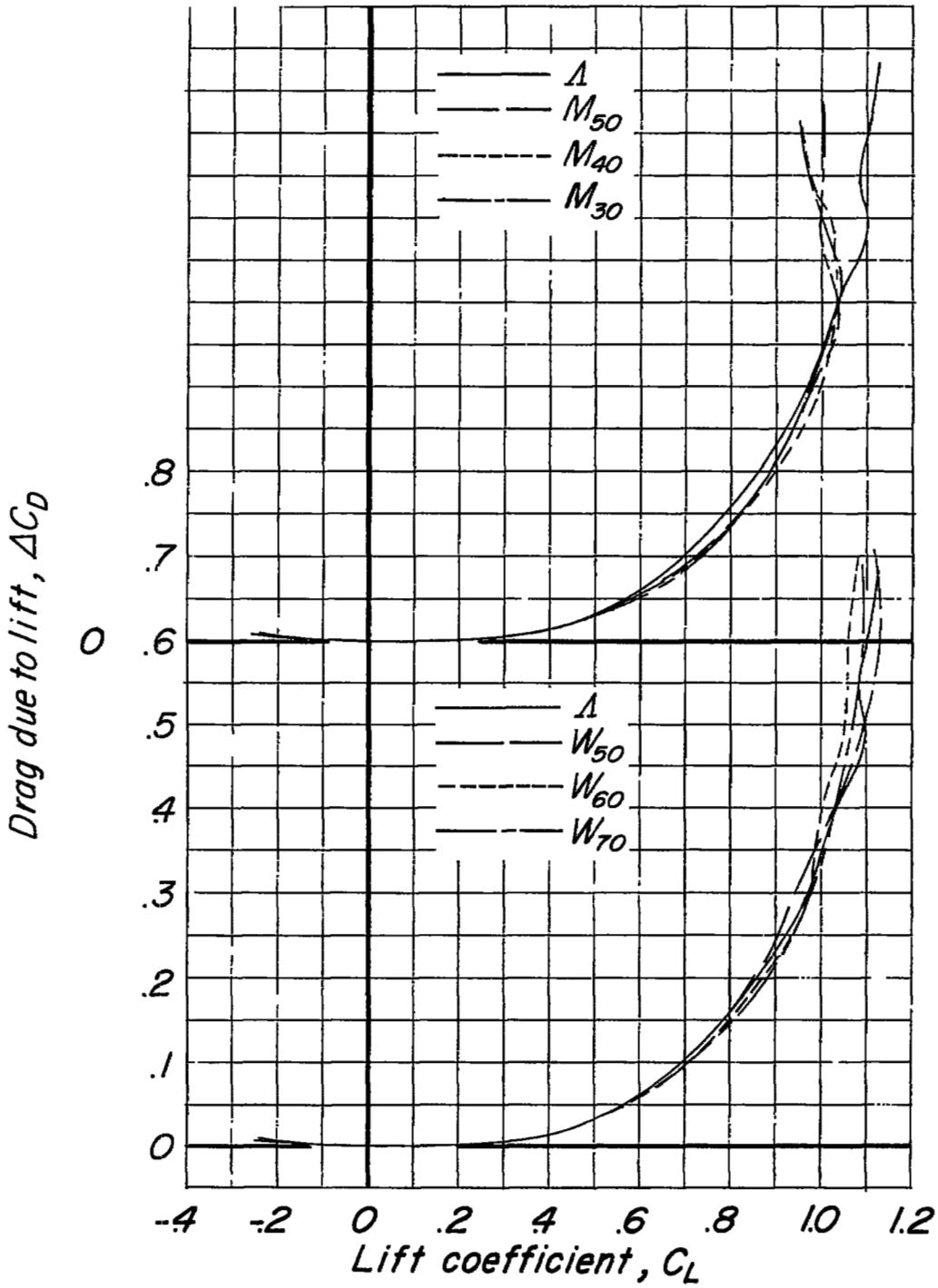

Figure 14.- Drag due to lift of model with various wings. Horizontal tail off.

[redacted]

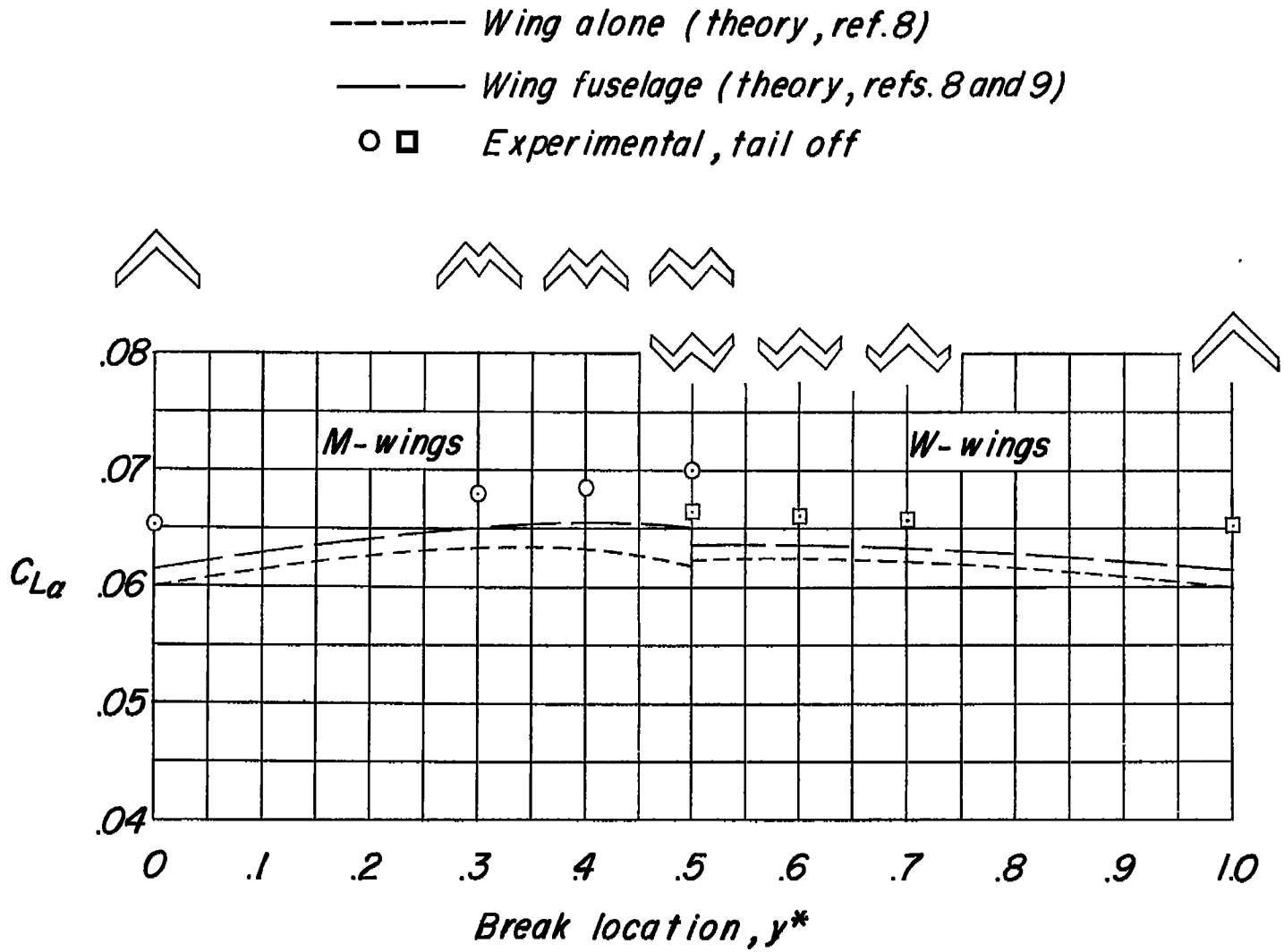

Figure 15.- Effect of break location on the lift-curve slope. $C_L = 0$.

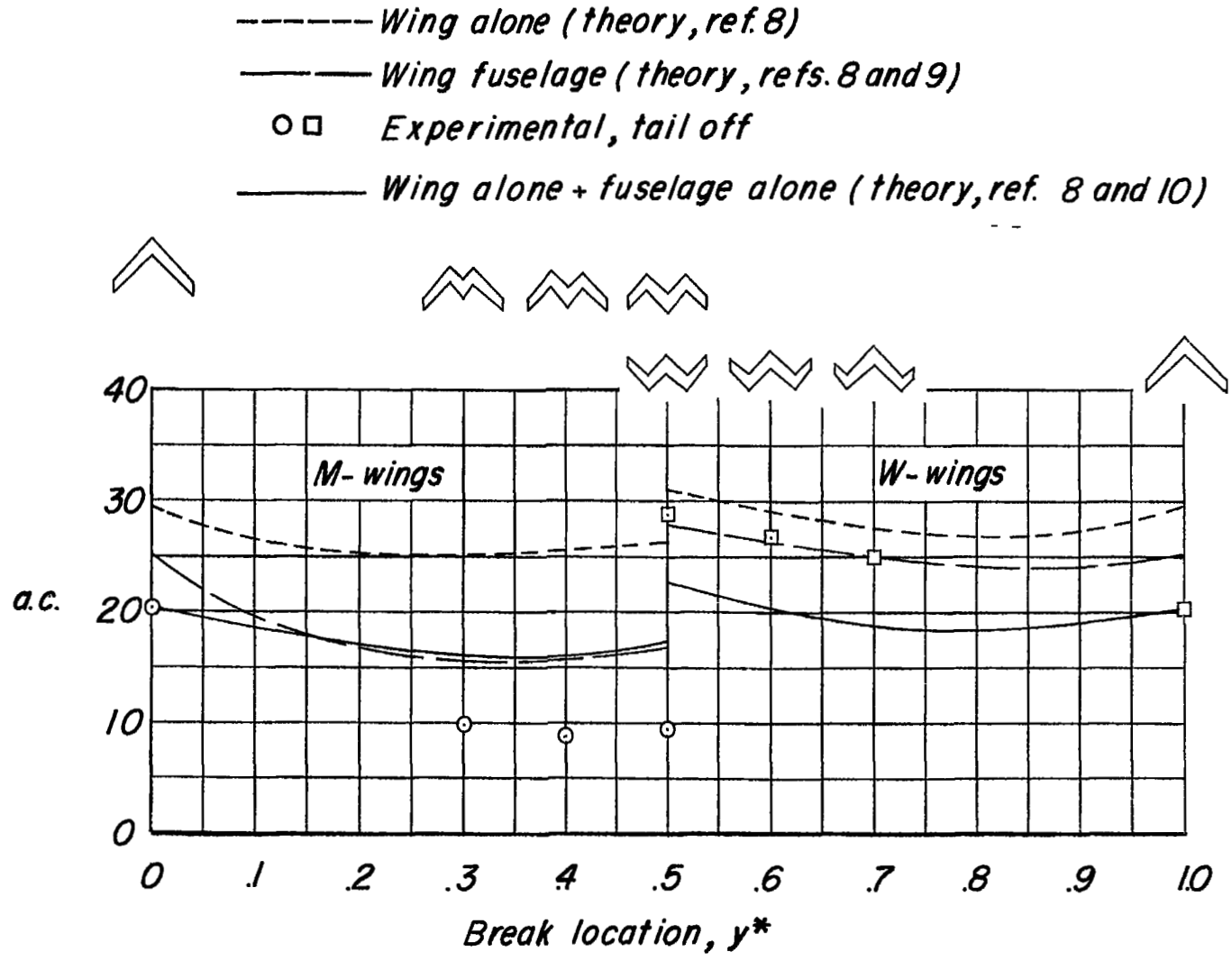

Figure 16.- Effect of break location on aerodynamic-center location. $C_L = 0$.

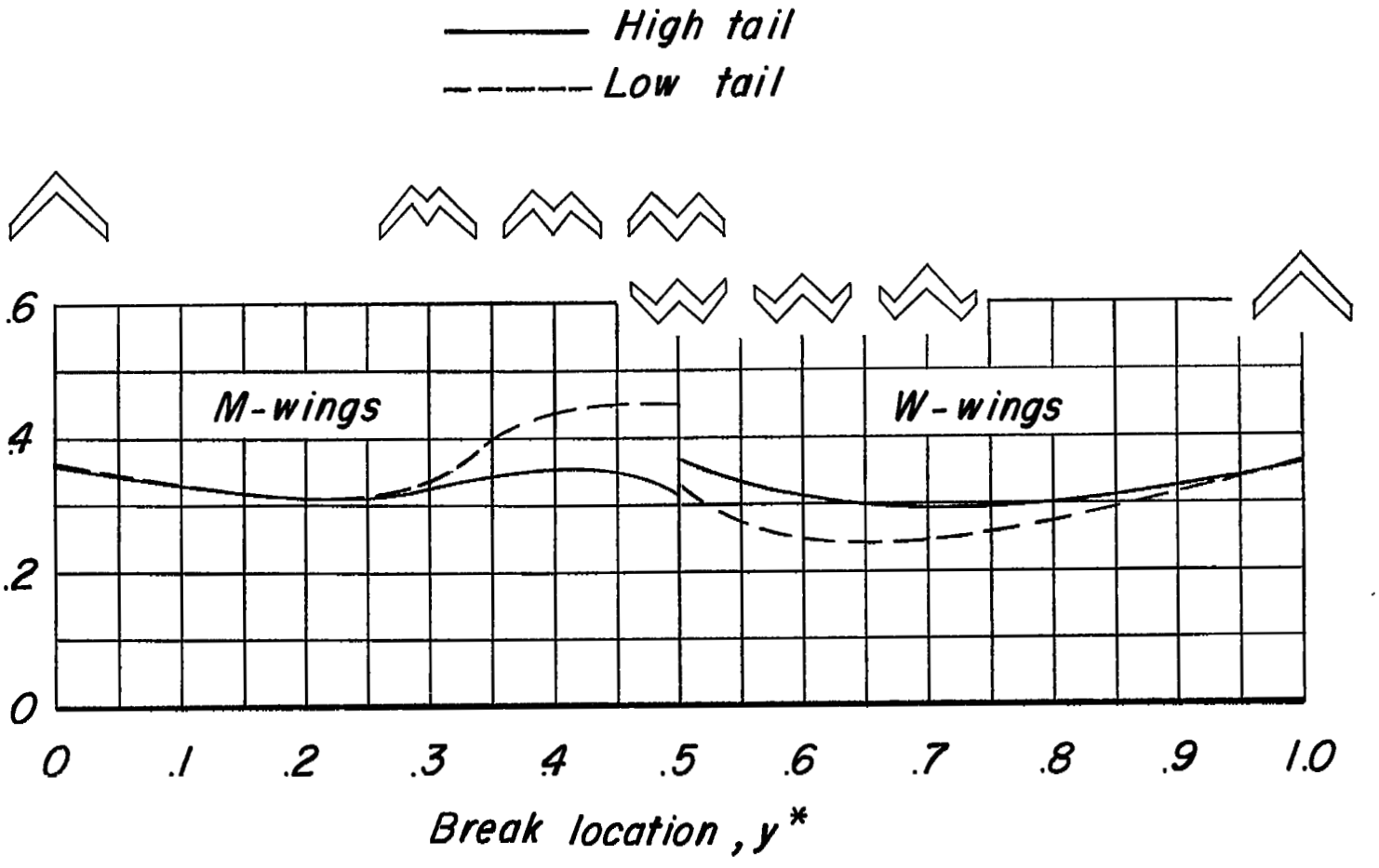

Figure 17.- Effect of break location on downwash parameter. $\alpha = 0$.

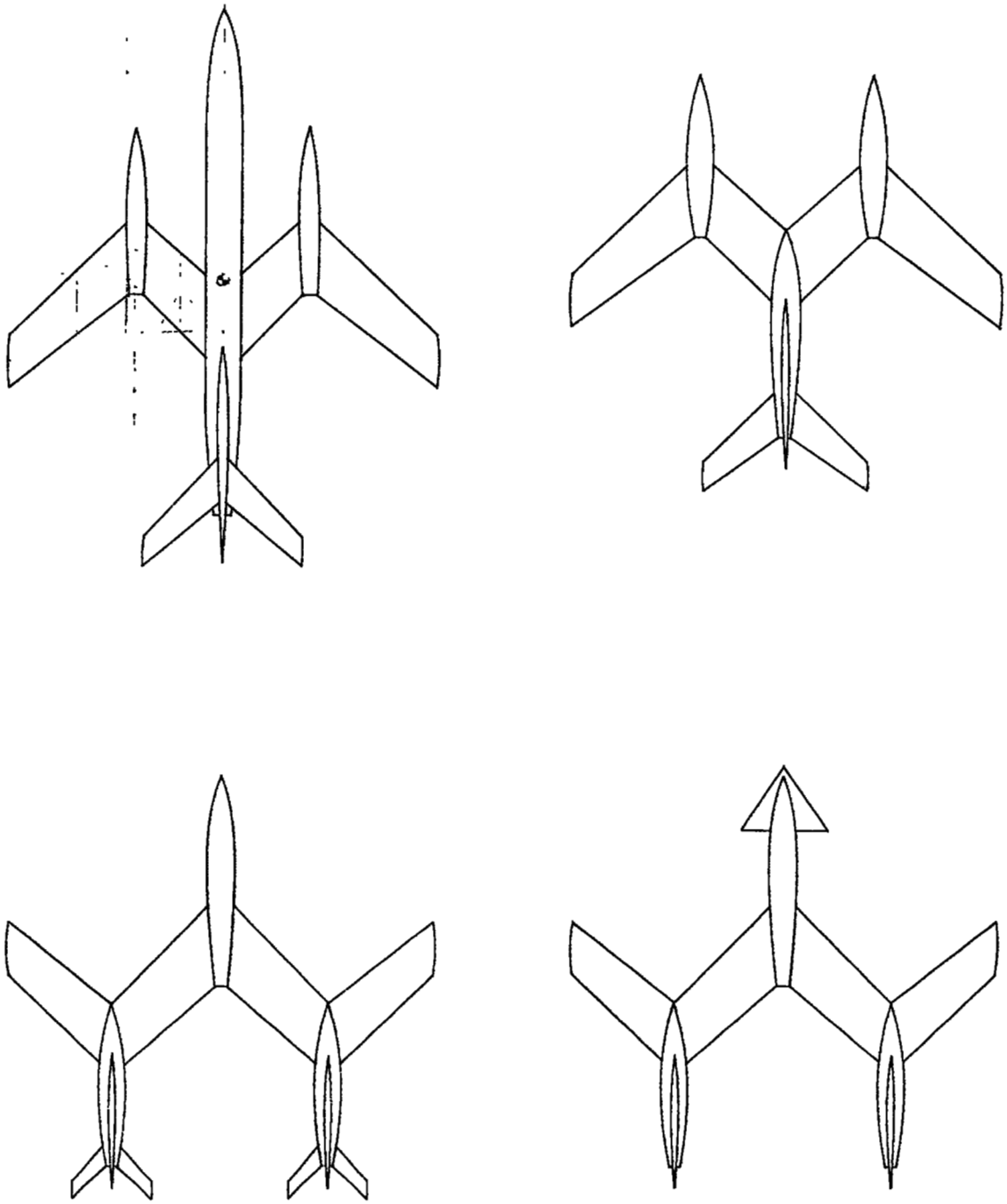

Figure 18.- Possible configurations.

NACA-Langley - 1-20-55 - 350